Molecular Biology of the Cell
Vol. 20, 3996–4009, September 15, 2009

Role for RACK1 Orthologue Cpc2 in the Modulation of Stress Response in Fission Yeast

Andrés Núñez, Alejandro Franco, Marisa Madrid,* Teresa Soto, Jero Vicente, Mariano Gacto, and José Cansado

Yeast Physiology Group, Department of Genetics and Microbiology, Facultad de Biología, University of Murcia, 30071 Murcia, Spain

Submitted May 13, 2009; Revised July 2, 2009; Accepted July 9, 2009
Monitoring Editor: Daniel J. Lew

The receptor of activated C kinase (RACK1) is a protein highly conserved among eukaryotes. In mammalian cells, RACK1 functions as an adaptor to favor protein kinase C (PKC)-mediated phosphorylation and subsequent activation of c-Jun NH_2-terminal kinase mitogen-activated protein kinase. Cpc2, the RACK1 orthologue in the fission yeast *Schizosaccharomyces pombe*, is involved in the control of G2/M transition and interacts with Pck2, a PKC-type protein member of the cell integrity Pmk1 mitogen-activated protein kinase (MAPK) pathway. Both RACK1 and Cpc2 are structural components of the 40S ribosomal subunit, and recent data suggest that they might be involved in the control of translation. In this work, we present data supporting that Cpc2 negatively regulates the cell integrity transduction pathway by favoring translation of the tyrosine-phosphatases Pyp1 and Pyp2 that deactivate Pmk1. In addition, Cpc2 positively regulates the synthesis of the stress-responsive transcription factor Atf1 and the cytoplasmic catalase, a detoxificant enzyme induced by treatment with hydrogen peroxide. These results provide for the first time strong evidence that the RACK1-type Cpc2 protein controls from the ribosome the extent of the activation of MAPK cascades, the cellular defense against oxidative stress, and the progression of the cell cycle by regulating positively the translation of specific gene products involved in key biological processes.

INTRODUCTION

Receptor of activated protein C kinase (RACK1) is a 36-kDa protein highly conserved in eukaryotic cells and a member of the family of proteins with WD repeats (McCahill *et al*., 2002). This group includes a large number of proteins involved in the regulation of key biological functions such as signal transduction, cell cycle control, vesicular trafficking, chromatin organization, and programmed cell death (Smith *et al*., 1999). Cryo-electron microscopy and x-ray crystallographic data indicate that RACK1 displays a β-propeller structure, with seven blades corresponding to the WD repeat domains, in a general conformation closely resembling the β-subunit structure of heterotrimeric G proteins (Sengupta *et al*., 2004; Chaudhuri *et al*., 2008; Coyle *et al*., 2009). RACK1 was initially identified by its ability to interact with protein kinase C isoforms, but later studies demonstrated that also binds in vivo other proteins related to signal transduction pathways, leading to the suggestion that it might act as scaffold to recruit elements involved in cell signaling (McCahill *et al*., 2002, Sengupta *et al*., 2004). In particular, mammalian RACK1 seems relevant to the regulation of angiogenesis, tumor growth, neuronal response, and apoptosis (McCahill *et al*., 2002). Recently, a direct relationship has been established between RACK1 and the c-Jun NH_2-terminal kinase (JNK) signal transduction pathway because RACK1 favors the protein kinase C (PKC)-mediated Ser129 phosphorylation and subsequent activation of the mitogen-activated protein (MAP) kinase JNK induced by phorbol esters, tumor necrosis factor-α, and UV radiation (López-Bergami *et al*., 2005).

Schizosaccharomyces pombe contains an orthologue of RACK1, named Cpc2, whose amino acid sequence shows ~70% identity with the human version (McLeod *et al*., 2000). The *cpc2*$^+$ gene was identified in fission yeast through its action on protein kinase Ran1/Pat1, which inhibits sexual development by regulating the transition from mitosis to meiosis (McLeod *et al*., 2000). Mutants lacking Cpc2 show distinct phenotypes such as delayed G2/M transition with increased cell size, defective G1 arrest under nitrogen deprivation, and inability to grow at high temperature (McLeod *et al*., 2000). Another relevant biological function of Cpc2/RACK1 is related to translation. This protein has been shown as a structural component of the 40S ribosomal subunit (Shor and McLeod, 2003; Baum *et al*., 2004; Coyle *et al*., 2009). Recent analyses of the Cpc2 orthologue Asc1 in *Saccharomyces cerevisiae* indicate a location close to the exit tunnel for mRNAs through an interaction that is dependent on WD domain I (Coyle *et al*., 2009). In *S. pombe*, the absence of Cpc2 decreases the synthesis of some proteins in a selective manner (Shor and McLeod, 2003). However, the exact role of RACK1/Cpc2/Asc1 as a regulator in translation remains to be established (Nilsson *et al*., 2004).

This article was published online ahead of print in *MBC in Press* (http://www.molbiolcell.org/cgi/doi/10.1091/mbc.E09–05–0388) on July 22, 2009.

* Present address: Paterson Institute for Cancer Research, University of Manchester, Manchester M20 4BX, United Kingdom.

Address correspondence to: Mariano Gacto (maga@um.es).

Abbreviations used: EMM2, Edinburgh minimal medium 2; GFP, green fluorescent protein; HA6H, epitope comprising hemagglutinin antigen plus six histidine residues; HA, hemagglutinin; MAPK, mitogen-activated protein kinase; PKC, protein kinase C; SAPK, stress-activated protein kinase; YES, yeast extract plus supplements.

Similar to RACK1, Cpc2 associates in vivo with Pck2, one of the two C-type protein kinases present in the fission yeast (Won *et al*., 2001). Also, it seems likely that Cpc2 may somehow regulate Pck2-dependent cell signaling in this yeast because the lethal effect of *pck2*$^+$ overexpression is attenuated by simultaneous overexpression of *cpc2*$^+$ (Won *et al*., 2001). In this context, several researchers, including ourselves, have shown that Pck2 is a member of the cell integrity pathway that regulates morphogenesis, cell wall construction, cytokinesis, and ion homeostasis (Ma *et al*., 2006; Barba *et al*., 2008). The key element of this transduction pathway is MAP kinase Pmk1, which is activated during cell separation and in response to many adverse conditions such as hyper- and hypo-osmotic stress, glucose withdrawal, presence of compounds disturbing the cell wall, and oxidative stress induced by hydroperoxides or pro-oxidant stressors (Madrid *et al*., 2006, 2007). In addition, *S. pombe* shows an MAP kinase pathway activatable by stress (SAPK), homologue to the metazoan SAPK, whose central element is MAPK Sty1, which results activated under various stressing conditions (Millar *et al*., 1995; Shiozaki and Russell, 1995; Degols *et al*., 1996; Soto *et al*., 2002). Once activated, Sty1 associates in vivo and phosphorylates Atf1, a leucine zipper domain transcription factor orthologue to ATF-2 in higher cells, which regulates gene expression determining the adaptive response of *S. pombe* to different stresses (Degols *et al*., 1996; Shiozaki and Russell, 1996; Wilkinson *et al*., 1996; Chen *et al*., 2003). Among the various phosphatases able to dephosphorylate Sty1 are tyrosine phosphatases Pyp1 and Pyp2, and serine-threonine phosphatases Ptc1 and Ptc2 (Hohmann, 2002). We have recently shown that Pyp1, Pyp2, and Ptc1, whose transcriptional activation is dependent on Sty1–Atf1 function, interact also with Pmk1 in vivo and may participate in its dephosphorylation, thus providing a first evidence for the existence of "cross-talk" between the two MAP kinase (MAPK) pathways in *S. pombe* (Madrid *et al*., 2007).

Extensive experimental evidence supports a high functional homology among the intracellular signaling pathways of the fission yeast and higher eukaryotes. This feature endows *S. pombe* with advantages as a suitable experimental model to study control mechanisms of general significance carried out by RACK1/Cpc2. In this article, we characterize the involvement of Cpc2 in the regulation of key signaling pathways of the fission yeast.

MATERIALS AND METHODS

Strains, Plasmids, and Growth Conditions

The *S. pombe* strains (Table 1) were grown with shaking at 28°C in either yeast extract plus supplements (YES) medium or Edinburgh minimal medium 2 (EMM2) (Moreno *et al*., 1991) with 2% of glucose, and supplemented with adenine, leucine, histidine, or uracil (100 mg/l; Sigma Aldrich, St. Louis, MO) depending on their particular requirements. Transformation of yeast strains was performed by the lithium acetate method (Moreno *et al*., 1991). Mutant strains were obtained by transformation or by mating and selecting diploids in EMM2 medium without supplements. Spores were purified by glusulase treatment (Soto *et al*., 2002) and allowed to germinate in EMM2 plus the appropriate requirements. Correct construction of strains was verified by polymerase chain reaction (PCR), and Western blot analyses (see below). Plasmid pREP3X-cpc2 was constructed to obtain strains expressing Cpc2 under the control of the full-strength thiamine repressible promoter. In brief, *cpc2*$^+$ open reading frame (ORF) was amplified by PCR using genomic *S. pombe* DNA as template and the oligonucleotides CPC2–5X (TATATCTCGAGATGCCAGAACAACTTGTGCTC, XbaI site is underlined) and CPC2–3X (TATATGGATCCTTACTTGGTAACTTGCCAGAC, BamHI site is underlined). The resulting ~1.4-kbp DNA fragment was digested with XbaI and BamHI and cloned into plasmid pREP3X. In experiments employing pREP3X-cpc2, the transformants were grown in EMM2 with or without thiamine (5 mg/l) for 12–24 h. To visualize the localization of a GFP-Pap1 fusion in cultures treated with either hydrogen peroxide or diethylmaleate (DEM), we used strains EHH14 and AN050 (Table 1), which harbor an integrated copy of the wild-type green fluorescent protein (GFP)-Pap1 chimeric gene under the control of the mid-strength thiamine repressible promoter *nmt1* (Madrid *et al*., 2004), both in wild-type and *cpc2*Δ backgrounds, respectively.

Gene Disruption and Epitope Tagging

The *cpc2*$^+$ null mutants were obtained by entire deletion of the corresponding coding sequence and its replacement with the KanMX6 cassette by PCR-mediated strategy using plasmid pFA6a-kanMX6 as template (Bahler *et al*., 1998). To construct strains expressing C-terminal 13-myc or GFP-tagged versions of either *pyp1*$^+$, *pyp2*$^+$, *ptc1*$^+$, *ptc3*$^+$, *pmp1*$^+$, *ctt1*$^+$, and *cpc2*$^+$, we used plasmids pFA6a-13Myc-kanMX6 and pFA6a-GFP-kanMX6, respectively (Bahler *et al*., 1998). Primer sequences used in each case are available upon request. Strains expressing genomic versions of Pmk1 fused to HA6H epitope at its C terminus in different genetic backgrounds were constructed either by transformation with integrative plasmid pIH-*pmk1*-ura (Madrid *et al*., 2006), or after random spore analysis of appropriate crosses. This procedure was also used to obtain strains expressing C-terminal HA6H-tagged versions of Sty1 or Atf1.

Site-directed Mutagenesis

A 2-kbp DNA fragment with the *cpc2*$^+$ ORF plus regulatory sequences was amplified by PCR employing the 5′-oligonucleotide CPC2GFP-5 (sequence CCTTATCTAGACCATACTTTCATATACGG; which hybridizes at positions −585 to −567 upstream of the *cpc2*$^+$ ATG start codon and contains a XbaI site), and the 3′-oligonucleotide CPC2GFP-3 (sequence CCTTAGGATCCCTCTTGGTAACTTGCCAGAC, which hybridizes at the 3′ end of *cpc2*$^+$ ORF and incorporates a BamHI site upstream of the TAA stop codon). The DNA fragment was then digested with XbaI and BamHI and cloned into integrative plasmid pIL-GFP to generate pIL-Cpc2-GFP, which incorporates a Cpc2 C-terminal fusion with the GFP tag, and contains the *S. pombe leu1*$^+$ gene as selectable marker. The Cpc2 R36D K38E mutant was created by the overlap extension method with the use of PCR (Higuchi *et al*., 1988). Two separate amplification reactions were performed with plasmid pIL-Cpc2-GFP as template with the use of a first pair of primers, CPC2GFP-5 and DE-3 (ATGATGGACT**C**GTCA**TC**AGAACCGGAAAG; the nucleotide substitutions are indicated in bold) and a second pair of primers, CPC2GFP-3 and DE-5 (CTTTCCGGTTCT**G**ATGAC**GA**GTCCATCAT; the nucleotide substitutions are indicated in bold). The two pairs of PCR products were purified by agarose gel electrophoresis, mixed, and subjected again to PCR with primers CPC2GFP-5 and CPC2GFP-3. The purified PCR product was purified, digested with XbaI and BamHI, and cloned into integrative plasmid pIL-GFP to generate pIL-Cpc2(DE)-GFP. Plasmids pIL-Cpc2-GFP and pIL-Cpc2(DE)-GFP were digested at the unique NruI site within *leu1*$^+$, and the linear fragments transformed into *cpc2*-disrupted strains. Transformants *leu1*$^+$ were obtained and the correct integration of the Cpc2-GFP fusion plus regulatory sequences was verified by sequencing and Western blot analysis.

Purification and Detection of Activated Pmk1-HA6H and Sty1-HA6H Proteins

To investigate Pmk1 activation under stress, we used log phase cell cultures (A_{600} of 0.5) growing at 28°C in YES medium that were then subjected to the appropriate treatment. In all cases, 30 ml of culture was harvested by centrifugation at 4°C, the cells washed with cold phosphate-buffered saline buffer, and the yeast pellets immediately frozen in liquid nitrogen for analysis. To analyze Pmk1 dual phosphorylation, total cell homogenates were prepared under native conditions employing chilled acid-washed glass beads and lysis buffer (10% glycerol, 50 mM Tris-HCl, pH 7.5, 150 mM NaCl, 0.1% Nonidet P40, plus specific protease and phosphatase inhibitor cocktails for fungal and yeast extracts [obtained from Sigma-Aldrich]). The lysates were cleared by centrifugation at 20,000 × *g* for 20 min. HA6H-tagged Pmk1 was purified by using nickel-nitrilotriacetic acid (Ni^{2+}-NTA)-agarose beads (QIAGEN, Valencia, CA), as reported previously (Soto *et al*., 2002). The purified proteins were resolved in 10% SDS-polyacrylamide gel electrophoresis (PAGE) gels, transferred to Hybond-ECL membranes (GE Healthcare, Chalfont St. Giles, Buckinghamshire, United Kingdom), and incubated with either mouse polyclonal anti-phospho-p42/44 (Cell Signaling Technology, Danvers, MA) or mouse monoclonal anti-hemagglutinin (HA) antibodies (clone 12CA5, loading control; Roche Molecular Biochemicals, Mannheim, Germany). To analyze tyrosine phosphorylation status in both Pmk1 and Sty1, cells were lysed into denaturing lysis buffer (6 M guanidine HCl, 0.1 M sodium phosphate, and 50 mM Tris-HCl, pH 8.0) as described by Shiozaki and Russell (1997), and HA6H-Pmk1 and HA6H-Sty1 fusions were purified after incubation with Ni^{2+}-NTA-agarose beads. After processing the purified proteins for Western blot analysis as described above, the membranes were hybridized with either a mouse monoclonal anti-phosphotyrosine (PY99; Santa Cruz Biotechnology) or mouse monoclonal anti-HA (loading control) antibodies. In all cases the immunoreactive bands were revealed with an anti-mouse horseradish peroxidase (HRP)-conjugated secondary antibody (Sigma-Aldrich) and the ECL system (GE Healthcare). Densitometric quantification of Western blot signals

Table 1. *S. pombe* strains used in this study

Strain	Genotype	Source/reference
MM1	h$^+$ *ade6-M216 leu1-32 ura4D-18*	Madrid *et al*. (2004)
MM2	h$^-$ *ade6-M210 leu1-32 ura4D-18*	Madrid *et al*. (2004)
AN001	h$^+$ *ade6-M216 cpc2::KanR leu1-32 ura4D-18*	This work
AN002	h$^-$ *ade6-M210 cpc2::KanR leu1-32 ura4D-18*	This work
MI200	h$^+$ *ade6-M216 pmk1-HA6H::ura4$^+$ leu1-32 ura4D-18*	Madrid *et al*. (2006)
MI201	h$^-$ *ade6-M210 pmk1-HA6H::ura4$^+$ leu1-32 ura4D-18*	Madrid *et al*. (2006)
AN100	h$^+$ *ade6-M216 cpc2::KanR pmk1-HA6H::ura4$^+$ leu1-32 ura4D-18*	This work
AN101	h$^-$ *ade6-M216 cpc2::KanR pmk1-HA6H::ura4$^+$ leu1-32 ura4D-18*	Madrid *et al*. (2006)
GB3	h$^+$ *ade6-M216 pck2::KanR pmk1-HA6H::ura4$^+$ leu1-32 ura4D-18*	Madrid *et al*. (2006)
AN150	h$^+$ *ade6-M216 pck2::KanR cpc2::KanR pmk1-HA6H::ura4$^+$ leu1-32 ura4D-18*	This work
TP319-13c	h$^-$ *pmk1::ura4$^+$ leu1-32 ura4D-18*	Toda *et al.* (1996)
AN160	h$^-$ *ade6-M216 cpc2::KanR pmk1::ura4$^+$ leu1-32 ura4D-18*	This work
MI212	h$^+$ *ade6-M216 pmp1::KanR pmk1-HA6H::ura4$^+$ leu1-32 ura4D-18*	Madrid *et al*. (2007)
AN170	h$^+$ *ade6-M216 cpc2::KanR pmp1::HygR pmk1-HA6H::ura4$^+$ leu1-32 ura4D-18*	This work
PP42	h$^-$ *ade6-M210 ppb1::ura4$^+$ leu1-32 ura4D-18*	P. Pérez
AN010	h$^-$ *ade6-M210 cpc2::KanR ppb1::ura4$^+$ leu1-32 ura4D-18*	This work
JM1521	h$^+$ *ade6-M216 his7-366 sty1-HA6H:: ura4$^+$ leu1-32 ura4D-18*	J. B. Millar
AN200	h$^+$ *ade6-M216 cpc2::KanR sty1-HA6H:: ura4$^+$ leu1-32 ura4D-18*	This work
MI709	h$^-$ *wis1DD-12myc::ura4$^+$ pmk1-HA6H::ura4$^+$ leu 1-32 ura4-D18*	Madrid *et al*. (2006)
MI713	h$^-$ *wis1DD-12myc::ura4$^+$ pmk1-HA6H::ura4$^+$ atf1:: ura4$^+$ leu 1-32 ura4-D18*	Madrid *et al*. (2006)
AN600	h$^-$ *wis1DD-12myc::ura4$^+$ pmk1-HA6H::ura4$^+$ cpc2::KanR leu 1-32 ura4-D18*	This work
MI701	h$^+$ *ade6-M216 pyp1-13myc:: KanR leu1-32 ura4D-18*	Madrid *et al*. (2006)
AN700	h$^+$ *ade6-M216 pyp1-13myc:: KanR cpc2::KanR leu1-32 ura4D-18*	This work
MI702	h$^+$ *pyp2-13myc:: ura4$^+$ leu1-32 ura4D-18*	J. B. Millar
AN400	h$^-$ *pyp2-13myc:: ura4$^+$ cpc2:: KanR leu1-32 ura4D-18*	This work
MI703	h$^+$ *ade6-M216 ptc1-13myc:: KanR leu1-32 ura4D-18*	Madrid *et al*. (2006)
AN500	h$^+$ *ade6-M216 ptc1-13myc:: KanR cpc2:: KanR leu1-32 ura4D-18*	This work
MI305	h$^+$ *ade6-M216 pmp1-GFP:: KanRleu1-32 ura4D-18*	Madrid *et al*. (2006)
AN020	h$^+$ *ade6-M216 pmp1-GFP:: KanR cpc2:: KanR leu1-32 ura4D-18*	This work
AN030	h$^+$ *ade6-M216 ptc3-13myc:: KanR leu1-32 ura4D-18*	This work
AN031	h$^+$ *ade6-M216 ptc1-13myc:: KanR cpc2:: KanR leu1-32 ura4D-18*	This work
MI213	h$^+$ *ade6-M216 pyp1::KanR pmk1-HA6H:: ura4$^+$ leu1-32 ura4D-18*	Madrid *et al*. (2007)
AN032	h$^+$ *ade6-M216 pyp1::KanR cpc2:: KanR pmk1-HA6H:: ura4$^+$ leu1-32 ura4D-18*	This work
JM1821	h$^-$ *ade6-M216 his7-366 atf11-HA6H:: ura4$^+$ leu1-32 ura4D-18*	J. B. Millar
AN300	h$^-$ *ade6-M216 atf11-HA6H:: ura4$^+$ cpc2:: KanR leu1-32 ura4D-18*	This work
1243	h$^-$ *ade6-M210 eIF2α(S52A):: ura4$^+$ leu1-32 ura4D-18*	Tvegård *et al.* (2007)
AN040	h$^-$ *ade6-M210 eIF2α(S52A):: ura4$^+$ atf11-HA6H:: ura4 leu1-32 ura4D-18*	This work
AN041	h$^-$ *ade6-M210 eIF2α(S52A):: ura4$^+$ atf11-HA6H:: ura4 cpc2:: KanR leu1-32 ura4D-18*	This work
TK107	h$^-$ *sty1:: ura4$^+$ leu 1-32 ura4-D18*	T. Kato
MI103	h$^+$ *ade6-M216 atf1:: ura4$^+$ leu1-32 ura4D-18*	Madrid *et al*. (2007)
EHH14	h$^-$ *his2 nmt41:pap1-GFP:: leu1$^+$ leu1-32 ura4D-18*	Madrid *et al*. (2004)
AN050	h$^-$ *his2 nmt41:pap1-GFP:: leu1$^+$ cpc2:: KanR leu1-32 ura4D-18*	This work
AN060	h$^+$ *ade6-M216 ctt1-GFP:: KanRleu1-32 ura4D-18*	This work
AN061	h$^+$ *ade6-M216 ctt11-GFP:: KanR cpc2::KanR leu1-32 ura4D-18*	This work
AN070	h$^+$ *ade6-M216 cpc2-GFP:: KanRleu1-32 ura4D-18*	This work
AN071	h$^+$ *ade6-M216 cpc2:: KanR cpc2-GFP::leu1$^+$ pmk1-HA6H:: ura4$^+$leu1-32 ura4D-18*	This work
AN072	h$^+$ *ade6-M216 cpc2:: KanR cpc2(R36D K38E)-GFP:: leu1$^+$ pmk1-HA6H:: ura4$^+$ leu1-32 ura4D-18*	This work
AN081	h$^+$ *ade6-M216 cpc2:: KanR cpc2-GFP:: leu1$^+$ atf1-HA6H:: ura4$^+$leu1-32 ura4D-18*	This work
AN082	h$^+$ *ade6-M216 cpc2:: KanR cpc2(R36D K38E)-GFP:: leu1$^+$ atf1-HA6H:: ura4$^+$ leu1-32 ura4D-18*	This work
AN091	h$^+$ *ade6-M216 cpc2:: KanR cpc2-GFP:: leu1$^+$ pyp1-13myc:: KanR pmk1-HA6H:: ura4$^+$ leu1-32 ura4D-18*	This work
AN092	h$^+$ *ade6-M216 cpc2:: KanR cpc2(R36D K38E)-GFP:: leu1$^+$ pyp1-13myc:: KanR pmk1-HA6H:: ura4$^+$ leu1-32 ura4D-18*	This work
AN102	h$^-$ *cpc2:: KanR cpc2-GFP:: leu1$^+$ pyp2-13myc:: ura4$^+$ leu1-32 ura4D-18*	This work
AN103	h$^-$ *cpc2:: KanR cpc2(R36D K38E)-GFP::leu1$^+$ pyp2-13myc:: ura4$^+$ leu1-32 ura4D-18*	This work

was performed using Molecular Analyst software (Bio-Rad Laboratories, Hercules, CA).

Purification and Detection of Atf1-HA6H

Atf1 protein was isolated by affinity precipitation on Ni^{2+}-NTA-agarose beads with cells extracts obtained under denaturing conditions as described above. The purified proteins were resolved in 6% SDS-PAGE gels, transferred to Hybond-ECL membranes, and incubated with a mouse anti-HA antibody (12CA5). In parallel, cell extracts were incubated with polyclonal rabbit anti-Cdc2 antibody (PSTAIR; Millipore, Billerica, MA) as a loading control.

Detection of Myc- and GFP-tagged Fusions

Cell extracts were prepared under native conditions (see above). The cleared lysates were resolved in 8 or 10% SDS-PAGE gels, depending on the relative size of the fusion protein, transferred to filters, and incubated with monoclonal mouse anti-c-myc antibody (clone 9E10; Roche Molecular Biochemicals) or polyclonal rabbit anti-GFP antibody (Cell Signaling Technology). Rabbit anti-Cdc2 antibody was used as loading control. Immunoreactive bands were detected using anti-mouse or anti-rabbit HRP-conjugated secondary antibodies (Sigma-Aldrich) and the SuperSignal system (Pierce Chemical, Rockford, IL).

Assays of Cell Sensitivity for Growth under Different Stresses

In plate assays, wild type and mutant strains of *S. pombe* were grown in YES liquid medium to an A_{600} of 0.6. Appropriate dilutions were spotted per duplicate on YES solid media containing 2% (wt/vol) bacto-agar (Difco, Detroit, MI) and supplemented with any of the following compounds: caspofungin (a kind gift from Merck, Darmstadt, Germany), $MgCl_2$ (Sigma-Al-

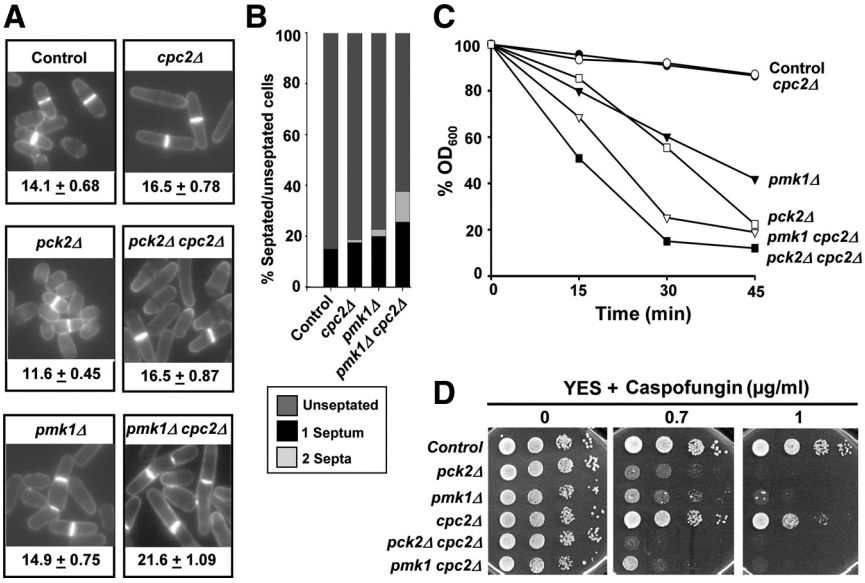

Figure 1. Role of Cpc2 in the regulation of cell size, septation, and cell wall integrity is independent of the Pmk1 MAPK pathway. (A) Cell morphology and size at division (micrometers ± SD) in strains MI200 (control), AN100 (*cpc2*Δ), GB3 (*pck2*Δ), AN150 (*pck2*Δ *cpc2*Δ), TP319–13c (*pmk1*Δ), and AN160 (*pmk1*Δ *cpc2*Δ), growing in EMM2 medium after staining with calcofluor white. (B) Septation status of the cells in the above cultures (n ≥ 400). (C) The same strains were grown in YES medium (OD_{600} = 0.5) and assayed for β-glucanase sensitivity by treatment with 100 μg/ml Zymolyase 20-T at 30°C. Cell lysis was monitored by measuring decay in OD_{600} at different incubation periods, and the results shown are the mean value of three independent experiments. (D) Cell survival in the presence of Caspofungin. Samples containing 10^4, 10^3, 10^2 or 10^1 cells of wild type and single- and double-mutant strains grown in YES medium were spotted onto YES plates supplemented with 0, 0.7, or 1 μg/ml caspofungin and incubated for 3 d at 28°C before being photographed.

drich), FK506 (cyclosporin; Alexis Biochemicals, San Diego, CA), potassium chloride (Sigma-Aldrich), sorbitol (Sigma-Aldrich), or hydrogen peroxide (Sigma-Aldrich). Plates were incubated at 28°C for 3 d and then photographed. When determining cell survival in liquid cultures, cells were grown in YES liquid medium to an A_{600} of 0.6 and treated with 5 mM hydrogen peroxide for 30 min. Then, cell samples were collected, appropriately diluted, and spread in triplicate onto YES plates. The viability of the cells was measured by their ability to form colonies after incubation at 28°C for 5 d. The survival fraction was calculated as a percentage relative to control samples that received no treatment.

β-1,3-Glucanase Sensitivity Assay

To analyze resistance to β-1,3-glucanase in different mutants, we followed the method of Loewith *et al.* (2000), with some modifications. Strains were grown in YES medium to an A_{600} of 0.6; washed with 10 mM Tris-HCl, pH 7.5, 1 mM EDTA, 1 mM β-mercaptoethanol; and incubated with vigorous shaking at 30°C in the same buffer supplemented with 100 μg/ml Zymolyase 20-T (Seikagaku America, Rockville, MD). Samples were taken every 15 min, and cell lysis monitored by measuring A_{600} decay.

Preparation and Fractionation of Polysomes

Polysomes were obtained as described previously (Shor and McLeod, 2003), with some modifications. Strains grown in YES medium (OD_{600} = 0.5) were treated with 100 μg/ml cycloheximide before centrifugation. The pelleted cells were washed, resuspended in lysis buffer (10 mM Tris-HCl, pH 7.5, 100 mM NaCl, 30 mM $MgCl_2$, and 100 μg/ml cycloheximide), and supplemented with a protease inhibitor cocktail (Sigma-Aldrich) and 0.5 U/μl RNAse inhibitor (RNasin; Ambion, Austin, TX). Total cell homogenates were obtained in a Fast-Prep instrument (Bio 101, Vista, CA) with chilled acid-washed glass beads, and the crude extracts clarified by centrifugation at 20,000 × *g* for 30 min. To show the polysome profile, 20 OD_{260} units of clarified extracts were applied to 11.2 ml of 7–47% (wt/vol) sucrose gradients in lysis buffer plus inhibitors and centrifuged in a SW41Ti rotor (Beckman Instruments, Fullerton, CA) at 4°C for 3.5 h at 40,000 rpm. Fractions of 600 μl were collected, and 50-μl aliquots were used to detect either Cpc2 or ribosomal protein L7 (internal control) by SDS-PAGE and Western blot analysis.

Northern Blot Analysis

Yeast cells grown in YES medium to an OD_{600} of 0.8, subjected to the appropriate stress treatment, and volumes of 50 ml of the cultures were recovered at different times. Total RNA preparations were obtained as described and resolved through 1.5% agarose-formaldehyde gels. Northern (RNA) hybridization analyses were performed as described previously (Soto *et al.*, 2002). The probes used were amplified by PCR and included: a 1.7-kbp fragment of the *atf1*$^+$ gene that was amplified with the 5′-oligonucleotide ATGTCCCCGTCTCCCGT and the 3′-oligonucleotide CTAGTACCCTAAATTGA; a 0.4-kbp fragment of the *gpx1*$^+$ gene amplified with the 5′-oligonucleotide TTCTACGACTTGGCT and the 3′-oligonucleotide ACACTCTCGATATCG; a 0.9-kbp fragment of the *trr1*$^+$ gene amplified with the 5′-oligonucleotide GTGACTCACAACAAG and the 3′-oligonucleotide TAATCGGTATCTTCC; a 2.1-kbp fragment of the *pyp2*$^+$ gene amplified with the 5′-oligonucleotide CCGAGAGCGTTTCTTGGA and the 3′-oligonucleotide AAGGGCTTGGAAGCCTGG; a 1-kbp fragment of the *pyp1*$^+$ gene amplified with the 5′-oligonucleotide GCTCCTTCGGGTTCATGT and the 3′-oligonucleotide CCTTGGCAAGCGATGTAA; a 1.5-kbp fragment of the *ctt1*$^+$ gene amplified with the 5′-oligonucleotide CGTCCCTGTTTACAC and the 3′-oligonucleotide GCTTCCTTGGAACAT; a 1.1-kbp fragment of the *tpx1*$^+$ gene amplified with the 5′-oligonucleotide ATGAGTTTGCAAATCGGT and the 3′-oligonucleotide CATAAGTGCTTGGAAAAGTACT; and a 1-kbp fragment of the *leu1*$^+$ gene amplified with the 5′-oligonucleotide TCGTCGTCTTACCAGGAG and the 3′-oligonucleotide CAACAGCCTTAGTAATAT. Ready-To-Go DNA labeling beads (GE Healthcare) was used for DNA labeling. To establish quantitative conclusions, the level of mRNAs was determined in a PhosphorImager (GE Healthcare) and compared with the internal control (*leu1*$^+$ mRNA).

Fluorescence Microscopy

To determine cell size at division and percentage of multiseptated cells, yeast strains were grown in EMM2 medium to an OD_{600} of 0.5 and stained with calcofluor white, which specifically stains cell wall and septum (Alfa *et al.*, 1993). A minimum of 400 septated cells were scored for each mutant. To localize the Pap1-GFP fusion, yeast cultures grown in EMM2 medium to an OD_{600} of 0.5 and treated with hydrogen peroxide (final concentration, 1–5 mM) or DEM (final concentration, 4 mM). Small aliquots (10 μl) of the yeast cultures were loaded onto poly L-lysine coated slides, and the remaining suspension was withdrawn by aspiration. A DM 4000B fluorescence microscope (Leica, Wetzlar, Germany) with 40× and 100× objectives was used, and images were captured with a cooled DC 300F camera and IM50 software (Leica), and then imported into PhotoShop CS3 (Adobe Systems, Mountain View, CA).

Reproducibility of Results

All experiments were repeated at least three times with similar results. Representative results are shown.

RESULTS

Cross-Talk between Cpc2 and the Pmk1 Cell Integrity Pathway

To study a possible role for Cpc2 in the functional Pmk1 cell integrity pathway, we first explored cell size, morphology, and septation in different mutants. As described previously, exponentially growing *cpc2*Δ cells are elongated (McLeod *et al.*, 2000; Figure 1A) and *pck2*Δ cells are somewhat short, whereas *pmk1*Δ cells are slightly longer than control cells and display a mild multiseptate phenotype (Toda *et al.*, 1996; Zaitsevskaya-Carter and Cooper, 1997; Figure 1A). Significantly, *cpc2*$^+$ deletion increased cell size at division in both *pck2*Δ and *pmk1*Δ cells (Figure 1A) and enhanced the separation defect due to *pmk1*$^+$ deletion (12% multiseptation in

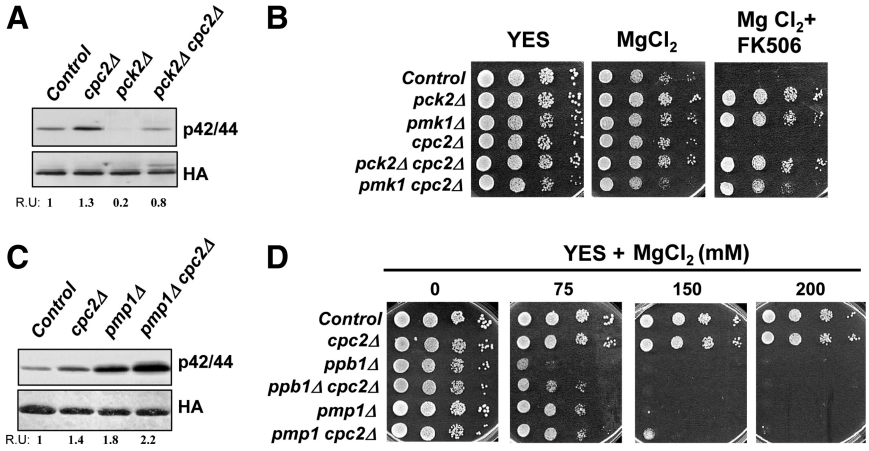

Figure 2. Cpc2 regulates chloride homeostasis in fission yeast alternatively to Pmk1. (A) Increased Pmk1 phosphorylation in *cpc2*Δ cells. Strains MI200 (*pmk1-HA6H*, control), AN100 (*pmk1-HA6H*, *cpc2*Δ), GB3 (*pmk1-HA6H*, *pck2*Δ), and AN150 (*pmk1-HA6H*, *pck2*Δ *cpc2*Δ) were grown in YES medium to mid-log phase, and Pmk1-HA6H was purified by affinity chromatography under native conditions. Activated and total Pmk1 was detected by immunoblotting with anti-phospho-p42/44 or anti-HA antibodies, respectively. (B) Chloride sensitivity assays for strains MI200 (control), GB3 (*pck2*Δ), TP319–13c (*pmk1*Δ), AN100 (*cpc2*Δ), AN150 (*pck2*Δ *cpc2*Δ), and AN160 (*pmk1*Δ *cpc2*Δ). After growth in YES medium, 10^4, 10^3, 10^2, or 10^1 cells were spotted onto YES plates supplemented with 0.2 M $MgCl_2$ or 0.2 M $MgCl_2$ plus 1 μg/ml FK506 and incubated for 3 d at 28°C before being photographed. (C) Strains MI200 (*pmk1-HA6H*, control), AN100 (*pmk1-HA6H*, *cpc2*Δ), MI212 (*pmk1-HA6H*, *pmp1*Δ), and AN170 (*pmk1-HA6H*, *pmp1*Δ *cpc2*Δ) were grown in YES medium to mid-log phase and total Pmk1-HA6H was purified and detected as described above. (D) Chloride sensitivity assays for strains MI200 (control), AN100 (*cpc2*Δ), PP42 (*ppb1*Δ), AN010 (*ppb1*Δ *cpc2*Δ), MI212 (*pmp1*Δ), and AN170 (*pmp1*Δ *cpc2*Δ). After growth in YES medium, cells were spotted onto YES plates supplemented with 75, 150, or 200 mM $MgCl_2$ and incubated for 3 d at 28°C.

double *cpc2*Δ *pmk1*Δ cells vs. 3 and 1% in either single *pmk1*Δ and *cpc2*Δ mutants, respectively) (Figure 1B). Sensitivity of the cell wall to digestion with β-glucanase in *cpc2*Δ *pck2*Δ or *cpc2*Δ *pmk1*Δ double mutants was higher than in *pck2*Δ or *pmk1*Δ cells (Figure 1C). Moreover, whereas *cpc2*Δ cells displayed some sensitivity toward the β-glucan synthase inhibitor caspofungin, this compound strongly affected cell growth in *pck2*Δ or *pmk1*Δ cells and particularly, in *cpc2*Δ *pck2*Δ and *cpc2*Δ *pmk1*Δ mutants (Figure 1D). Together, these results suggest that Cpc2 participates in the regulation of cell size, septation and cell wall integrity in an alternative manner or in addition to the Pmk1 pathway.

In human cells, RACK1 is required for PKC to phosphorylate JNK and increase its degree of activation (López-Bergami *et al*., 2005). Because fission yeast Cpc2 is also able to interact with Pck2 (Won *et al*., 2001), this precedent prompted us to perform a comparative analysis of basal MAPK activity in control versus *cpc2*Δ, *pck2*Δ, and *pck2*Δ *cpc2*Δ cells expressing a HA6H-tagged version of Pmk1, and by using an anti-p42/44 antibody that detects dual phosphorylation of Pmk1 at threonine and tyrosine residues (Madrid *et al*., 2006). As shown in Figure 2A, a moderate but reproducible increase in basal Pmk1 phosphorylation was evident in *cpc2*Δ cells compared with control cells. As described previously (Barba *et al*., 2008), *pck2*$^+$ deletion induced a very strong decrease in basal Pmk1 phosphorylation (Figure 2A). Notably, the basal level of Pmk1 phosphorylation was higher in *pck2*Δ *cpc2*Δ cells than in the single *pck2*Δ mutant (Figure 2A), suggesting that Cpc2 negatively regulates Pmk1 downstream to Pck2.

In *S. pombe*, calcineurin and Pmk1 play antagonistic roles in chloride homeostasis, and Pmk1 hyperactivation leads to strong sensitivity to this anion (Sugiura *et al*., 1998). Unexpectedly, cells lacking *cpc2*$^+$ did not show growth inhibition in rich medium supplemented with 0.2 M $MgCl_2$ (Figure 2B), whereas the *vic*-negative phenotype (*vic*, viable in the presence of FK506 and chloride; Ma *et al*., 2006) of the *cpc2*$^+$-deleted mutant was rescued by additional deletion of *pck2*$^+$ or *pmk1*$^+$genes (Figure 2B). These results point to Cpc2 as negative regulator of chloride homeostasis in a way that is independent of Pmk1 and/or calcineurin. In agreement with this prediction, a *cpc2*Δ *pmp1*Δ double mutant strain, which shows a higher Pmk1 activity than its parental single mutant counterparts (Figure 2C), displayed some growth in medium with higher concentration of $MgCl_2$ than the *pmp1*Δ mutant (Figure 2D). Moreover, disruption of *cpc2*$^+$ in a *ppb1*Δ strain (devoid of the catalytic subunit of calcineurin phosphatase; Yoshida *et al*., 1994) clearly increased tolerance against chloride anion compared with the single *ppb1*Δ mutant strain (Figure 2D). Hence, Cpc2 plays a role as a negative regulator for chloride homeostasis alternatively to Pmk1 in fission yeast.

Cpc2 Is Important for Both Pmk1 and Sty1 Tyrosine Dephosphorylation in Growing Cells and under Stress

The level of Pmk1 phosphorylation increases in a quick and transient manner when *S. pombe* is subjected to a salt-induced osmostress with KCl (Madrid *et al*., 2006). As shown in Figure 3A (top), the stress-induced Pmk1 activation in a strain deleted in *cpc2*$^+$ was maintained for longer times than in control cells and, as described above, exhibited a moderate increase in basal Pmk1 phosphorylation (Figure 3A, top). On the contrary, ectopic expression of the *cpc2*$^+$ gene in *cpc2*Δ cells caused a clear reduction in the levels Pmk1 phosphorylation both in growing cells and in response to hyperosmotic stress (Figure 3B). The positive role of Cpc2 in Pmk1 deactivation was also evident under other stressful situations such as oxidative stress with hydrogen peroxide (Figure 3C) or cell wall synthesis inhibition with caspofungin. Importantly, the basal and the stress induced Pmk1 phosphorylation levels were also higher in *cpc2*Δ than in control cells when using a specific anti-phosphotyrosine antibody (pY99) (Figure 3A, bottom). Moreover, deletion of *cpc2*$^+$ also resulted in increased basal level of Sty1 tyrosine phosphorylation and delayed deactivation kinetics under osmostress (Figure 3D). Together, these results suggest that Cpc2 acts as a negative regulator of the tyrosine phosphorylation status of both Pmk1 and Sty1 MAPKs.

Cpc2 Positively Regulates the Protein Levels of Pyp1 and Pyp2 Tyrosine Phosphatases

Recently, we described that MAPK Sty1 is essential for proper deactivation of Pmk1 under hypertonic stress in a process regulated by transcription factor Atf1 through the action of tyrosine phosphatases Pyp1 and Pyp2, and serine/

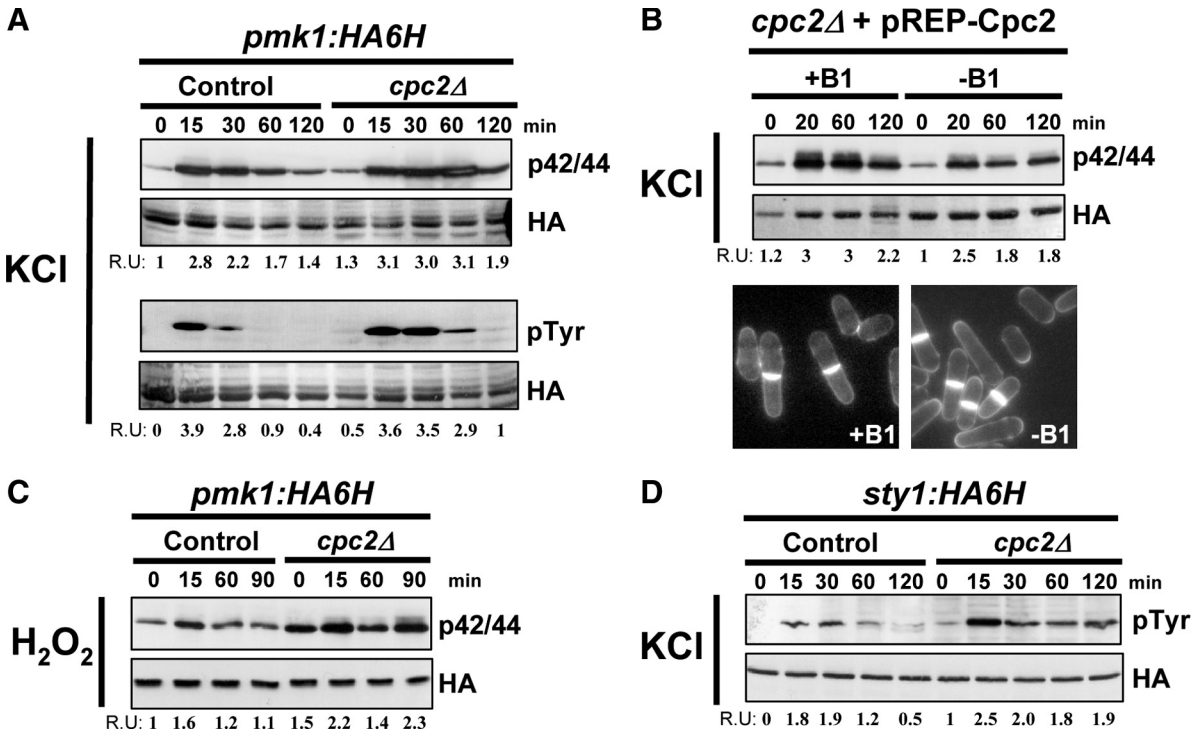

Figure 3. Cpc2 negatively regulates phosphorylation of Pmk1 and Sty1 MAPKs in growing and stressed cells. (A) Top, Strains MI200 (*pmk1-HA6H*, control), and AN100 (*pmk1-HA6H*, *cpc2*Δ), were grown in YES medium to mid-log phase and treated with 0.6 M KCl. At timed intervals Pmk1-HA6H was purified by affinity chromatography, and the activated and total Pmk1 was detected by immunoblotting with anti-phospho-p42/44 or anti-HA antibodies, respectively. Bottom, in the same experiment, Pmk1 phosphorylation was detected by immunoblotting with anti-phosphotyrosine antibody. (B) Strain AN100 (*pmk1-HA6H*, *cpc2*Δ) transformed with pREP-*cpc2*$^+$ plasmid was grown for 18 h in the presence (+B1) or absence (−B1) of thiamine and treated with 0.6 M KCl. At different times, Pmk1-HA6H was purified and the activated, and total Pmk1 was detected as described in A. Cell morphology was analyzed by fluorescence microscopy. (C) Strains MI200 (*pmk1-HA6H*, control) and AN100 (*pmk1-HA6H*, *cpc2*Δ) were grown in YES medium to mid-log phase, treated with 1 mM H_2O_2, and the activated and total Pmk1 was detected as described in A. (D) Strains JM1521 (*sty1-HA6H*, control) and AN200 (*sty1-HA6H*, *cpc2*Δ) were grown in YES medium to mid-log phase and treated with 0.6 M KCl. At timed intervals, Sty1-HA6H was purified by affinity chromatography and the activated and total Sty1 was detected by immunoblotting with anti-phosphotyrosine antibody or anti-HA antibodies, respectively.

threonine phosphatase Ptc1 (Madrid *et al*., 2007). Ptc3, another serine/threonine phosphatase, has been also involved in this control (Takada *et al*., 2007), whereas Pmp1, a dual-specificity phosphatase, seems involved in Pmk1 inactivation only in growing cells and during cell separation (Madrid *et al*., 2007). The results obtained so far strongly suggested that the observed increase in both the basal and the osmostress-induced phosphorylation of Pmk1 and Sty1 in *cpc2*Δ cells might be due to a deficit in the synthesis of any of the above-mentioned phosphatases. To test this interpretation, we undertook two experimental approaches on the bases of earlier findings. We showed previously that osmostress-induced Pmk1 activation/deactivation in a strain expressing a hyperactive version of Wis1 MAPKK (*wis1DD*), which prompts the constitutive activation of Sty1 (Shiozaki *et al*., 1998), is lower than in control cells due to increased synthesis of Pyp1, Pyp2, and Ptc1 (Madrid *et al*., 2007). Therefore, if somehow Cpc2 would positively regulate the levels of these phosphatases, then deletion of the *cpc2*$^+$ gene in a *wis1DD* background should rescue the defective Pmk1 activation observed in stressed cultures of the single *wis1DD* mutant. Results shown in Figure 4A indicate this first prediction is correct, because Pmk1 activation by salt stress is much higher in *cpc2*Δ *wis1DD* cells than in *wis1DD* cells, although not as much as in *cpc2*Δ *atf1*Δ cells. Second, we analyzed Pyp1–13myc, Pyp2–13myc, Ptc1–13myc, Ptc3–13myc, and Pmp1-GFP protein levels in exponentially growing control and *cpc2*Δ cultures and after being subjected to a hypertonic stress. As shown in Figure 4B, Pyp1 protein levels during growth were lower in the *cpc2*Δ mutant than in the control strain, whereas Pyp2, Pmp1, Ptc1, and Ptc3 levels were unaffected by the absence of Cpc2. However, upon osmostress, both Pyp1 and Pyp2, but not Pmp1, Ptc1, or Ptc3, were down-regulated in *cpc2*Δ mutant compared with control cells (Figure 4B). Moreover, the positive role of Cpc2 in modulating Pyp2 protein levels was also proved in *S. pombe* cells subjected to other stresses like oxidative treatment with hydrogen peroxide or heat shock (Figure 4C). Importantly, Pmk1 basal phosphorylation in *pyp1*Δ *cpc2*Δ cells was very similar to that of the single *pyp1*Δ mutant, but higher than in *cpc2*Δ cells (Figure 4D). As a whole, these results strongly suggest that in fission yeast Cpc2 acts as a positive regulator of Pyp1 and Pyp2 protein levels. In this scenario, the hyperactivation of Pmk1 and Sty1 observed in growing *cpc2*Δ cells is a consequence of the defect in the protein levels of Pyp1, whereas defective Pyp1 and Pyp2 levels account for the slow MAPK deactivation observed under stress.

Atf1 Level Is Positively Regulated by Cpc2

In fission yeast the stress-induced expression of *pyp1*$^+$ and *pyp2*$^+$ genes is regulated by Sty1 through Atf1 forming a negative-feedback loop (Degols *et al*., 1996; Shiozaki and Russell, 1996; Wilkinson *et al*., 1996). Hence, we considered

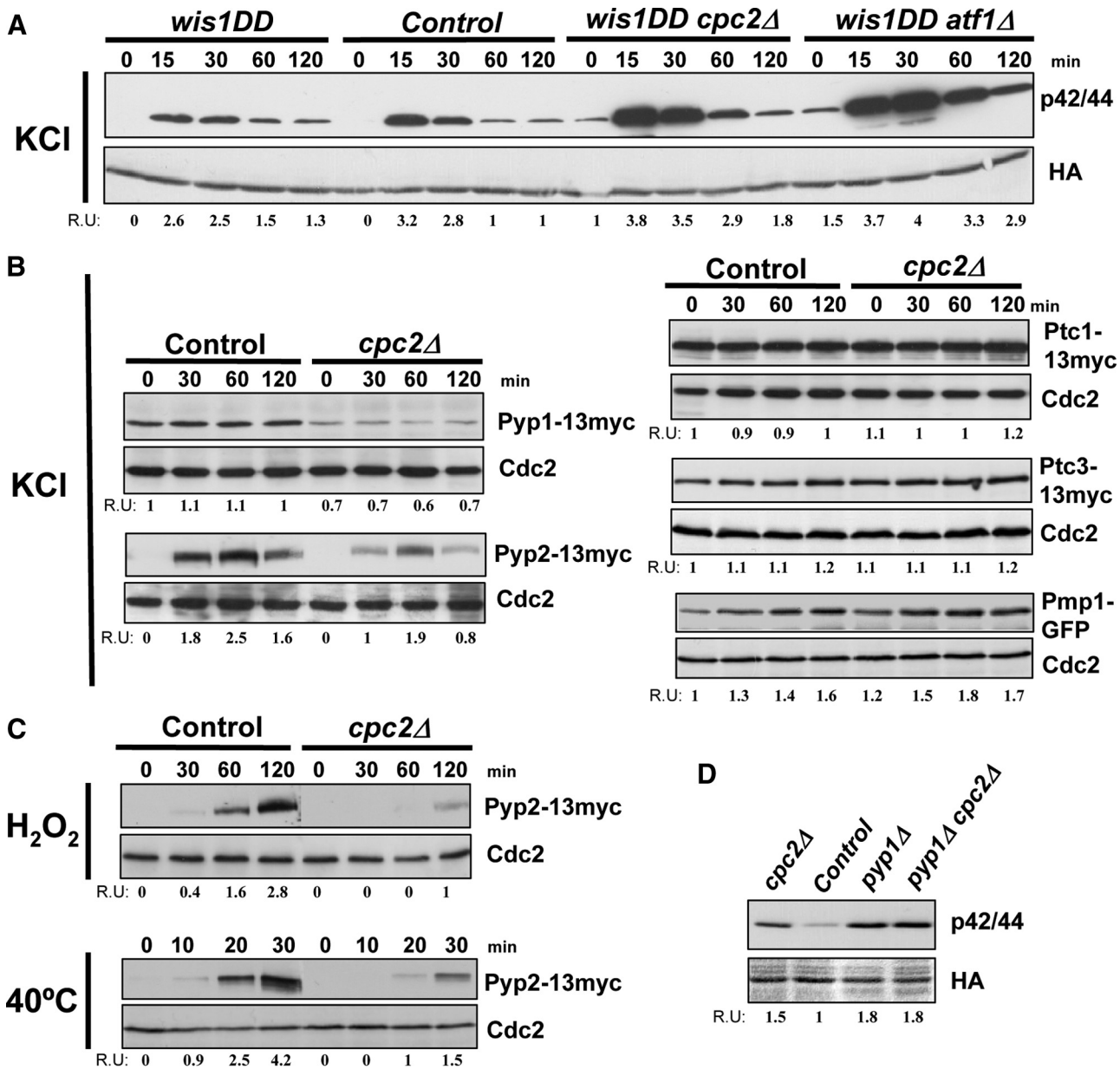

Figure 4. Cpc2 acts as a positive regulator of Pyp1 and Pyp2 tyrosine phosphatases protein levels. (A) Deletion of the *cpc2*$^+$ gene in a *wis1DD* background rescues the defective Pmk1 activation in single *wis1DD* mutant. Strains MI200 (*pmk1-HA6H*, control), MI709 (*pmk1-HA6H*, *wis1DD*), AN600 (*pmk1-HA6H*, *wis1DD cpc2*Δ), and MI713 (*pmk1-HA6H*, *wis1DD atf1*Δ) were grown in YES medium to mid-log phase and treated with 0.6 M KCl. At the times indicated, aliquots were harvested and Pmk1-HA6H was purified by affinity chromatography. Activated Pmk1 was detected by immunoblotting with anti-phospho-p42/44 and total Pmk1 with anti-HA antibodies. (B) Protein levels of different MAPK phosphatases. The strains MI701 (*pyp1–13myc*, control) and AN700 (*pyp1–13myc*, *cpc2*Δ), MI702 (*pyp2–13myc*, control) and AN400 (*pyp2–13myc*, *cpc2*Δ), MI703 (*ptc1–13myc*, control) and AN500 (*ptc1–13myc*, *cpc2*Δ), AN030 (*ptc3–13myc*, control), and AN031 (*ptc3–13myc*, *cpc2*Δ), MI305 (*pmp1-GFP*, control) and AN020 (*pmp1-GFP*, *cpc2*Δ) were grown in YES medium to mid-log phase and treated with 0.6 M KCl. Total extracts were obtained from aliquots harvested at the times indicated, and fusions to 13-myc and GFP were detected by immunoblotting with either anti-c-myc or anti-GFP antibodies, respectively, whereas anti-Cdc2 antibody was used for loading control. (C) Defective synthesis of Pyp2 in *cpc2*Δ cells subjected to other stresses. Strains MI702 (*pyp2–13myc*, control) and AN400 (*pyp2–13myc*, *cpc2*Δ) were grown as described above and treated with 1 mM H_2O_2 (top) or incubated at 40°C (bottom). Aliquots were harvested at the times indicated and Pyp2–13myc was detected by immunoblotting with anti-c-myc antibody. Anti-Cdc2 antibody was used for loading control. (D) The basal Pmk1 phosphorylation in *pyp1*Δ *cpc2*Δ cells is similar to that of the single *pyp1*Δ mutant. Strains MI200 (*pmk1-HA6H*, control), AN100 (*pmk1-HA6H*, *cpc2*Δ), MI213 (*pmk1-HA6H*, *pyp1*Δ), and AN032 (*pmk1-HA6H*, *pyp1*Δ *cpc2*Δ), were grown as indicated previously and Pmk1-HA6H was purified by affinity chromatography under native conditions. Activated and total Pmk1 was detected by immunoblotting with anti-phospho-p42/44 or anti-HA antibodies, respectively.

the possibility that the decreased Pyp1 and Pyp2 synthesis in stressed-*cpc2*Δ cells might result from a defect in the synthesis of Atf1 itself. In this context, we determined Atf1 protein levels in control and *cpc2*Δ cells expressing a genomic copy of the *atf1*$^+$ gene tagged with two copies of the HA epitope and six histidine residues, and after being subjected to a

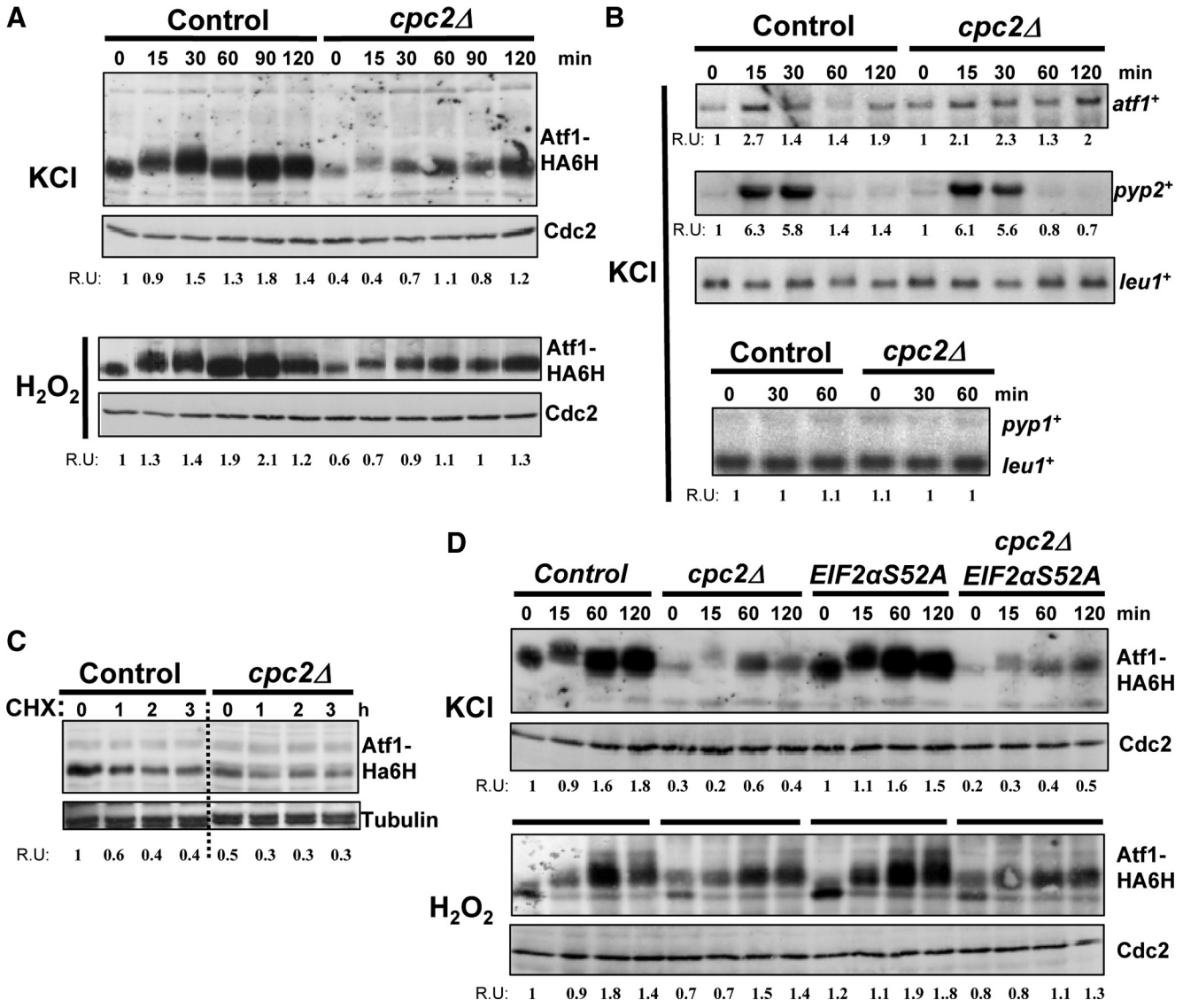

Figure 5. The protein level of Atf1 is positively regulated by Cpc2. (A) Strains JM1821 (*atf1-HA6H*, control) and AN300 (*atf1-HA6H*, *cpc2*Δ) were grown in YES medium to mid-log phase and treated with either 0.6 M KCl (top) or 1 mM H_2O_2 (bottom). Aliquots were harvested at different times, and Atf1 was purified from cell extracts by affinity chromatography, and detected by immunoblotting with anti-HA antibody. Anti-Cdc2 antibody was used for loading control. (B) Strains JM1821 and AN300 were grown at 28°C in YES medium to mid-exponential phase and treated with 0.6 M KCl for the times indicated. Total RNA was extracted, denatured, transferred to nylon membranes, and hybridized with ^{32}P-labeled probes for *atf1*$^+$, *pyp2*$^+$, *pyp1*$^+$, and *leu1*$^+$ (loading control). (C) These same strains were grown in YES medium (OD_{600} = 0.5) and treated with 100 μg/ml cycloheximide for the times indicated. Purified Atf1 was detected by immunoblotting with anti-HA antibody, whereas anti-α-tubulin antibody was used as loading control. (D) EIF2α is not involved in the control of Atf1 translation by Cpc2. Strains JM1821 (*atf1-HA6H*, control), AN300 (*atf1-HA6H*, *cpc2*Δ), AN040 (*atf1-HA6H*, *EIF2α-S52A*), and AN041 (*atf1-HA6H*, *EIF2α-S52A cpc2*Δ) were grown in YES medium and treated with either 0.6 M KCl (top) or 1 mM H_2O_2 (bottom). Atf1 from each sample was purified by affinity chromatography and detected by immunoblotting with anti-HA antibody. Anti-Cdc2 antibody was used for loading control.

saline stress with KCl. As shown in Figure 5A (top), *cpc2*$^+$ deletion prompted a clear decrease in Atf1 levels as compared with control cells in both growing and osmostressed cells. This defect was also evident in cultures under oxidative stress with hydrogen peroxide (Figure 5A, bottom). In contrast, because Atf1 positively regulates its own expression at a transcriptional level (Wilkinson *et al*., 1996), the defective Atf1 levels observed in *cpc2*Δ cells might result from a deficit in the expression of *atf1*$^+$ mRNA. To further investigate this approach we estimated *atf1*$^+$mRNA levels in control versus *cpc2*Δ cells under saline stress. As Figure 5B shows, *atf1*$^+$ mRNA levels were unaffected by the absence of Cpc2 in both cases. Remarkably, although Atf1 levels are lower in *cpc2*Δ cells, the salt induced expression of both *pyp2*$^+$ and *pyp1*$^+$ mRNAs was similar to control cells (Figure 5B).

The decreased Atf1 protein levels in *cpc2*Δ cells might result from a decreased stability. To address this point we determined the half-life of Atf1 in control versus *cpc2*Δ mutant strains growing in rich medium after the addition of cycloheximide, which blocks translation. As shown in Figure 5C, the half-life of Atf1 was very similar in control and *cpc2*Δ cells (~2 h). These results indicate that Cpc2 likely exerts a positive regulation on Atf1, Pyp1, and Pyp2 expres-

sion at a translational level by inducing the translation of their correspondent mRNAs.

In fission yeast, phosphorylation of the initiation factor EIF2-α at Ser-52 (Ser-51 in other eukaryotic cells) is critical for the inhibition of general protein synthesis by down-regulating the initiation of translation in response to multiple stresses (Zhan *et al*., 2002). To investigate a possible cross-talk between Cpc2 and EIF2-α phosphorylation for the control of Atf1 translation under stress conditions, we disrupted the *cpc2*$^+$ gene in a strain bearing a nonphosphorylatable alanine instead of Ser-52 in EIF2-α (EIF2-αS52A; Tvegård *et al*., 2007). As can be seen in Figure 5D, the absence of phosphorylation at Ser52 in EIF2-α did not noticeably affect Atf1 translation in response to either osmotic or oxidative stress, which remained similar to that of control cells. Moreover, both the basal and stress-induced synthesis of Atf1 was similarly compromised in *cpc2*Δ and *cpc2*Δ EIF2-αS52A cells (Figure 5D). Therefore, these data support a role for Cpc2 as positive regulator of Atf1 translation which is independent on EIF2-α function.

Cellular Response against Hydrogen Peroxide Stress Is Partially Compromised in cpc2Δ Cells

S. pombe strains lacking Sty1 or Atf1 are strongly sensitive to various stresses (Millar *et al*., 1995; Shiozaki and Russell, 1995; Shiozaki and Russell, 1996; Wilkinson *et al*., 1996). We examined the growth of control, *sty1*Δ, *atf1*Δ, and *cpc2*Δ strains on solid media supplemented with either KCl (saline osmostress), sorbitol (nonsaline osmostress), or hydrogen peroxide (oxidative stress), to ascertain whether defective synthesis of Atf1 in *cpc2*Δ mutant affected cell survival under stress. Contrary to *sty1*Δ or *atf1*Δ mutants, *cpc2*Δ cells did not show enhanced growth inhibition by KCl or sorbitol, although a mild growth defect was observed in the presence of 1, 5, 2 mM hydrogen peroxide that was less severe than in *atf1*Δ cells (Figure 6A). A similar result was observed when liquid cultures treated with 5 mM hydrogen peroxide were used (Figure 6B).

Transcription factor Pap1 is required for cell survival of fission yeast under oxidative stress (Vivancos *et al*., 2006), and its activity is regulated at the level of cellular localization. In growing cells Pap1 resides mainly in the cytoplasm but, in response to hydrogen peroxide, undergoes a reversible oxidation of critical cysteine residues and accumulates into the nucleus to favor the increased transcription of essential genes for defense against oxidative stress (Vivancos *et al*., 2006). Under moderate to high concentrations of hydrogen peroxide (naturally occurring, for example, in response to glucose arrest) nuclear accumulation of Pap1 is delayed until the expression of Atf1-dependent genes promotes its conversion to the active oxidized conformation that translocates into the nucleus and enhances Pap1-dependent gene expression (Madrid *et al*., 2004; Vivancos *et al*., 2006). Consequently, we analyzed the cellular location of Pap1 in strains EHH14 (control) and AN050 (*cpc2*Δ) after being treated with 1 mM hydrogen peroxide. These strains express a genomic copy of an N-terminal GFP-tagged version of Pap1 under the control of a mid-strength thiamine repressible promoter (Vivancos *et al*., 2004). As described previously (Vivancos *et al*., 2004), nuclear accumulation of activated Pap1 was maximal after 40–50 min of treatment and slowly decreased thereafter (Figure 6C). However, *cpc2*$^+$ disruption provoked a clear delay in nuclear translocation of Pap1 (~30 min as average of three independent experiments; Figure 6C), and the same effect was also observed when using higher doses of the oxidant (5 mM; Figure 6D). This defect was not due to a difference in protein expression, because Pap1 levels were similar in control and in *cpc2*Δ cells. Moreover, the kinetics of Pap1 nuclear accumulation was identical in both types of cells after treatment with pro-oxidant DEM, which induces a nonreversible Pap1 structural modification unrelated to that induced by hydrogen peroxide (Castillo *et al*., 2002; Figure 6D). Hence, the timing for nuclear accumulation of Pap1 results specifically delayed in *cpc2*Δ cells by oxidative stress with hydrogen peroxide. To further investigate this effect, we analyzed by Northern blot experiments the comparative expression of several genes which are induced in a Sty1-Atf1 and/or Pap1-dependent manner in response to hydrogen peroxide in control and in *cpc2*Δ cells. As shown in Figure 7, the

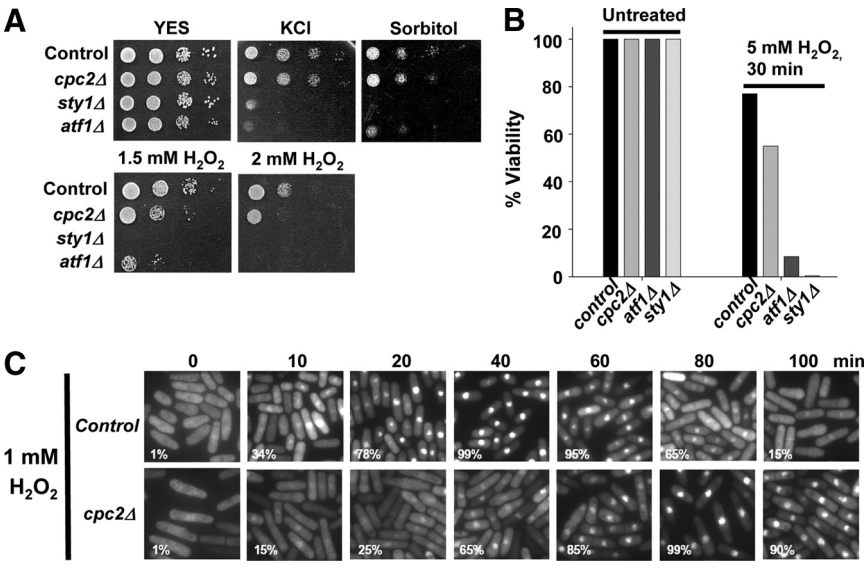

Figure 6. Cellular defense against hydrogen peroxide is defective in the absence of Cpc2. (A) Cell viability assays in solid medium were performed for strains MI200 (control), AN100 (*cpc2*Δ), TK107 (*sty1*Δ), and MI103 (*atf1*Δ). After growth in YES medium, 10^4, 10^3, 10^2, or 10^1 cells were spotted onto YES plates supplemented with either 0.6 M KCl, 1.2 M sorbitol, or 1.5–2 mM H_2O_2 and incubated for 4 d at 28°C before being photographed. (B) Cell viability assays in liquid medium for the above strains after growth in YES liquid medium (OD_{600} = 0.5) and treatment with 5 mM H_2O_2 for 30 min before seeding in YES plates. Survival was estimated as percentage of colony forming units relative to untreated cultures. The experiment was repeated three times with similar results. (C) Nuclear accumulation of GFP-Pap1 is delayed in *cpc2*Δ cells. Strains EHH14 (GFP-Pap1; control) and AN150 (GFP-Pap1, *cpc2*Δ), expressing a GFP-Pap1 fusion under the control of the nmt1-promoter, were grown in EMM2 medium to an OD_{600} = 0.5 and treated with 1 mM H_2O_2. Samples were taken at different times, and the percentage of cells with nuclear accumulation of GFP-Pap1 was determined by fluorescence microscopy. Results shown correspond to one representative experiment.

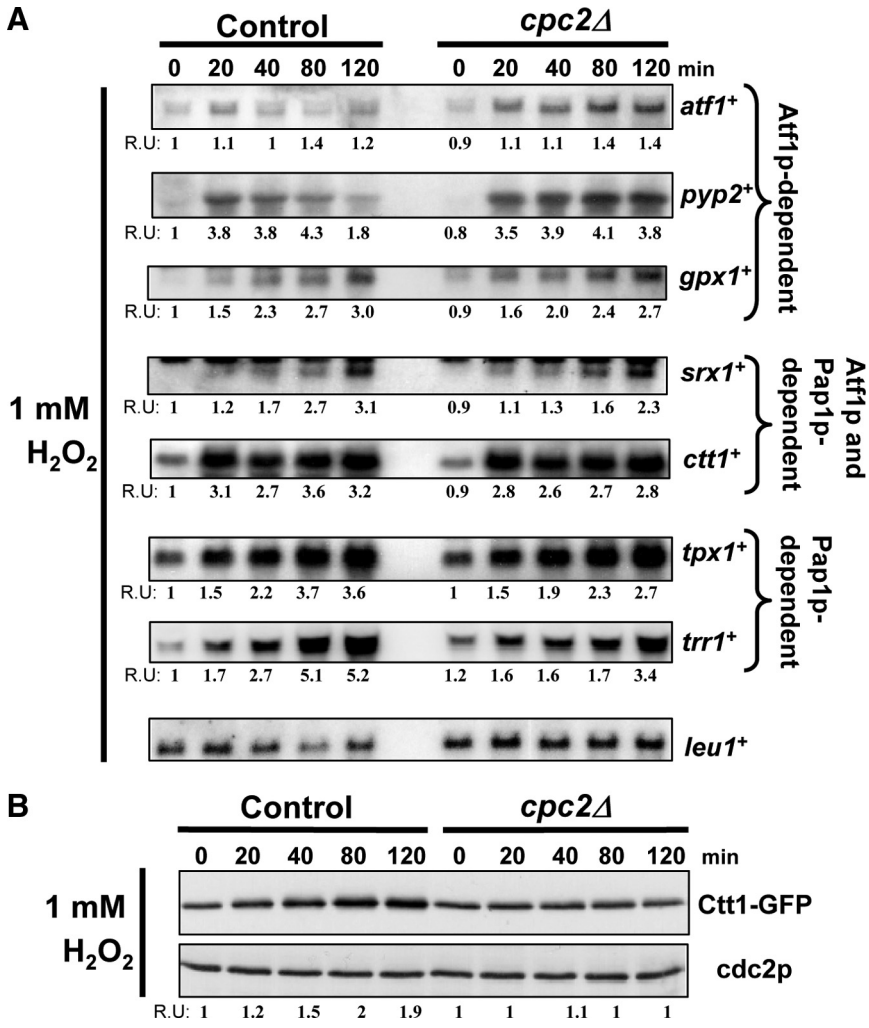

Figure 7. Cpc2 modulates *S. pombe* response to oxidative stress at both transcriptional and translational levels. (A) Induced expression of Pap1-dependent genes in response to hydrogen peroxide is delayed in *cpc2*Δ cells. Strains MI200 (control) and AN100 (*cpc2*Δ) were grown in YES medium to early log phase and treated with 1 mM H_2O_2 for the times indicated. Total RNA was extracted from each sample and 20 μg resolved in 1.5% agarose formaldehyde gels. The denatured RNAs were transferred to nylon membranes and hybridized with ^{32}P-labeled probes for *atf1*$^+$, *pyp2*$^+$, *gpx1*$^+$, *srx1*$^+$, *ctt1*$^+$, *tpx1*$^+$, *trr1*$^+$, and *leu1*$^+$ (loading control). (B) Increased synthesis of cytoplasmic catalase in response to hydrogen peroxide is blocked in *cpc2*Δ cells. Strains AN060 (control; *ctt1-GFP*) and AN061 (*cpc2*Δ, *ctt1-GFP*) were grown in YES medium and treated with 1 mM H_2O_2 for the times indicated. Total extracts were obtained and Ctt1-GFP fusion was detected by immunoblotting with anti-GFP antibodies. Anti-Cdc2 antibody was used for loading control.

transcriptional induction of Atf1-dependent genes like *atf1*$^+$ itself, *pyp2*$^+$, or *gpx1*$^+$ (encoding H_2O_2 scavenger glutathione peroxidase; Yamada *et al*., 1999) was not significantly affected by *cpc2*$^+$ deletion in exponentially growing cultures treated with 1 mM hydrogen peroxide, indicating that the moderate levels of Atf1 present in *cpc2*Δ cells support a correct transcriptional response. Under such conditions, a very slight decrease was observed in *cpc2*Δ cells compared with control cells in the transcriptional activation of genes like *srx1*$^+$ (sulfiredoxin; Quinn *et al*., 2002) and *ctt1*$^+$ (cytoplasmic catalase; Degols and Russell, 1997), whose expression is dependent on the activity of both Atf1 and Pap1 transcription factors (Quinn *et al*., 2002) (Figure 7A). In contrast, the induction kinetics of Pap1-dependent genes, like *tpx1*$^+$ (encoding thioredoxin peroxidase, Vivancos *et al*., 2006) and, most notably *trr1*$^+$ (thioredoxin reductase; Benko *et al*., 1998), was significantly retarded in a *cpc2*Δ background (Figure 7A), which is congruent with the delay in nuclear translocation of Pap1 (Figure 6C). However, such delay in H_2O_2-treated *cpc2*Δ cells remained unexplained on the bases of a transcriptional defect in the induced expression of Atf1-dependent genes. Thus, we analyzed the cellular levels of cytoplasmic catalase (Ctt1), which is involved in the detoxifying activity against oxidative stress in eukaryotic cells, in control and *cpc2*Δ cultures treated with 1 mM H_2O_2. As shown in Figure 7B, the increased Ctt1 synthesis observed in H_2O_2-treated control cells was absent in the *cpc2*Δ mutant, indicating a role for Cpc2 in the modulation of the intracellular level of cytoplasmic catalase under these conditions. These results suggest that Cpc2 is important in *S. pombe* to positively regulate the cellular defense against high doses of hydrogen peroxide at a translational level by favoring the synthesis of enzymes such as Ctt1, whose detoxifying activity is essential to allow Pap1-dependent gene expression.

Localization of Cpc2 at the Ribosome Is Essential to Regulate Pyp1, Pyp2, and Atf1 Protein Levels

A work by Coyle *et al*. (2009) has recently demonstrated that two evolutionary conserved charged amino acids on one side of the β-propeller structure of Asc1, the *S. cerevisiae* RACK1 orthologue, Arg38 and Lys40 (Arg36 and Lys38 in fission yeast), are responsible for RACK1 association with the 40S subunit of the ribosome in vivo. To analyze the biological significance of the ribosome localization of Cpc2 in fission yeast we constructed strains expressing either wild type or R36D K38E variant of Cpc2 fused to the green fluorescent protein at its C terminus, in a *cpc2*Δ background (see *Materials and Methods*). As shown in Figure 8A, both Cpc2-GFP and Cpc2(DE)-GFP fusions localized at the cell cytoplasm, similarly to a genomic Cpc2-GFP version expressed from is natural locus, and were expressed at nearly the same level (Figure 8B). However, the cytoplasmic distri-

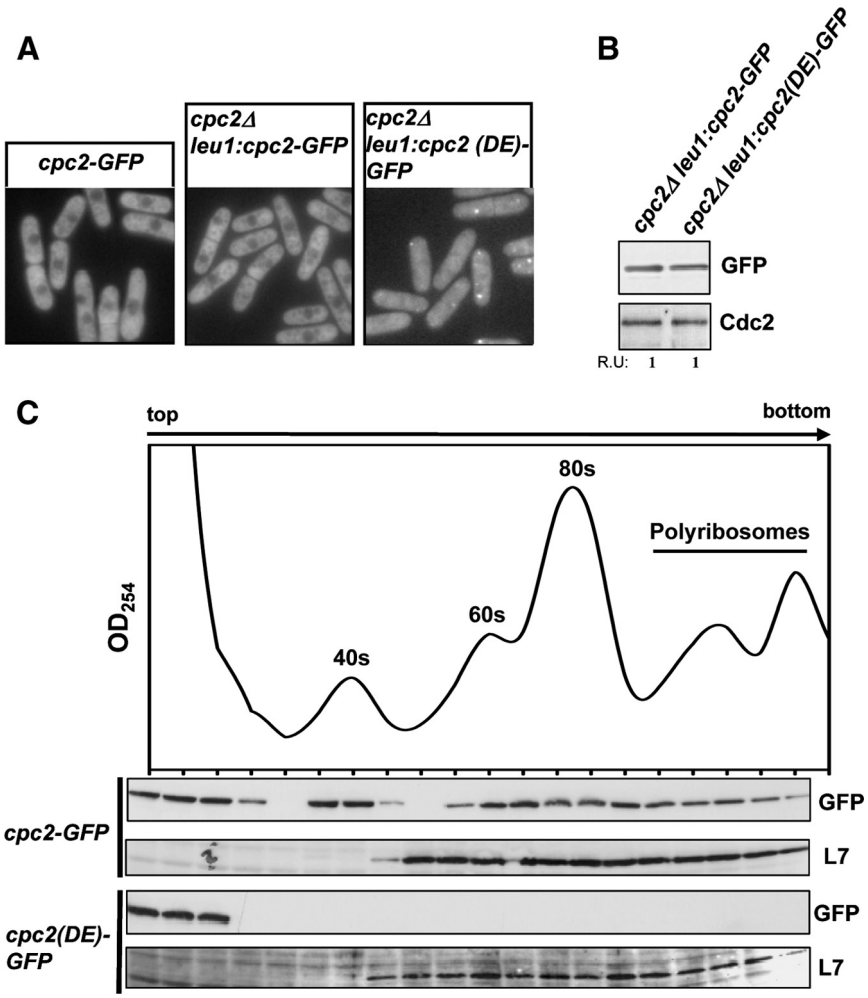

Figure 8. Construction of a *S. pombe* strain expressing a Cpc2 version unable to bind the ribosome in vivo. (A) Subcellular localization of Cpc2 variants. Mid-log phase cells of strains AN070 (*cpc2-GFP*, control), AN071 (*leu1:cpc2-GFP*, *cpc2*Δ), and AN072 (*leu1:cpc2(DE)-GFP*, *cpc2*Δ) growing in YES medium were visualized by fluorescence microscopy. (B) The Cpc2-GFP and Cpc2(DE)-GFP fusions are expressed at a similar level. GFP fusions were detected in total cell extracts from strains AN071 (*leu1:cpc2-GFP*, *cpc2*Δ) and AN072 (*leu1:cpc2(DE)-GFP*, *cpc2*Δ) by immunoblotting with anti-GFP antibodies. Anti-Cdc2 antibody was used for loading control. (C) Polysome Western blot analysis for in vivo ribosome binding. Strains AN071 and AN072 were grown in YES medium to early log phase, treated with cycloheximide, and the whole cell extracts processed for polysome analysis by velocity sedimentation on a 7–47% (wt/vol) sucrose gradient. After fractionation, the absorbance profile for each fraction was measured at 254 nm. A typical result is shown, with fractions corresponding to soluble (top), 40S, 60S, 80S, and polyribosomes. Aliquots from each fraction were resolved by SDS-PAGE and the elution profile for Cpc2-GFP or Cpc2 (DE)-GFP was determined by Western blot analysis with anti-GFP antibody. Anti-L7 antibody was used as an internal ribosomal control.

bution of Cpc2(DE)-GFP was more diffuse, and some punctate spots were visible throughout the cells (Figure 8A). Regardless, analysis of the distribution of both Cpc2-GFP and Cpc2(DE)-GFP by sucrose gradient fractionation of polyribosomes isolated from growing cells indicated that, contrary to wild-type cells, R36D K38E mutation in Cpc2 disrupted almost completely its ability to associate with ribosomes in vivo, with >95% of free, unbound protein (Figure 8C). Importantly, an increase in basal Pmk1 phosphorylation was evident in *cpc2*Δ cells expressing Cpc2(DE)-GFP compared with those expressing Cpc2-GFP (Figure 9A). These results suggest that Cpc2 localization at the ribosome is critical to negative regulate of Pmk1 activity in growing cells. Indeed, similar to *cpc2*Δ cells, a strain expressing Cpc2(DE)-GFP fusion was defective in Pmk1 deactivation under stress (Figure 9A), due to a decrease in the protein levels of both Pyp1 and Pyp2 tyrosine phosphatases (Figure 9B). Atf1 protein levels in both growing cells and in cultures subjected to either osmotic saline or oxidative stresses were also down-regulated in the Cpc2(DE) mutant (Figure 9C). As a whole, these results confirm that in fission yeast ribosome binding of Cpc2 is essential to positively regulate the translation efficiency of Pyp1, Pyp2, and Atf1. Finally, we also noticed that *cpc2*Δ cells expressing wild-type Cpc2-GFP, but not Cpc2(DE)-GFP, recovered their normal cell size at division (Figure 9D), indicating that Cpc2 binding to the ribosome is important to control the G2/M transition of the cell cycle in fission yeast.

DISCUSSION

In eukaryotic cells, RACK1 is a scaffold protein involved in a myriad of signal transduction pathways. However, the role of the fission yeast orthologue Cpc2 as a modulator of the signal transduction machinery had not been investigated in detail earlier. Similar to RACK1, Cpc2 was reported to interact in vivo with the PKC orthologue Pck2 (Won *et al.*, 2001). Also, others and ourselves showed that Pck2 is a member of the Pmk1 cell integrity MAPK pathway in fission yeast (Ma *et al.*, 2006; Barba *et al.*, 2008), suggesting that Cpc2 might be an integral part of this MAPK cascade. However, several lines of evidence obtained in this work indicate that, contrary to our initial prediction, Cpc2 is not a member of the Pmk1 signaling pathway. First, the cell separation and cell wall integrity defects described previously as associated to deletion of members of the cell integrity MAPK module (Toda *et al.*, 1996; Zaitsevskaya-Carter and Cooper, 1997) are exacerbated in a *cpc2*Δ background. Second, the fact that cell size at division is higher in both *cpc2*Δ *pck2*Δ and *cpc2*Δ *pmk1*Δ double mutants than in *pck2*Δ or *pmk1*Δ single mutants supports that the role of Cpc2 in the control of G2/M transition in the fission yeast is independent on Pmk1 activity. Third, and most important, whereas RACK1 functions in mammalian cells as an adaptor for MAPK JNK phosphorylation at Ser129 by PKC, which is required for JNK activation in response to several agents (López-Bergami *et al.*, 2005), in *cpc2*Δ cells of fission yeast both the basal and the stress

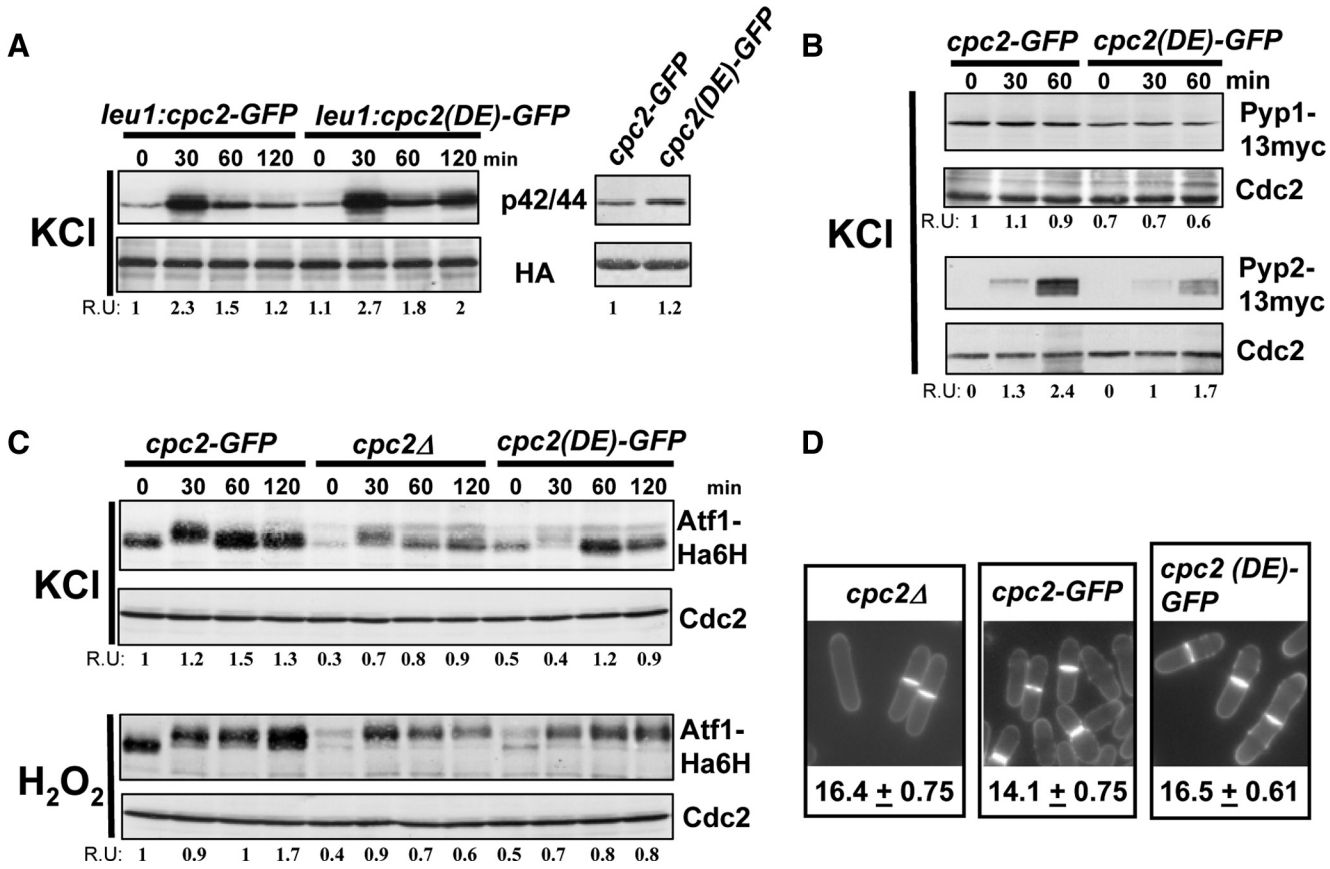

Figure 9. Ribosome binding of Cpc2 is essential to positively regulate the translation efficiency of Pyp1, Pyp2, and Atf1 in fission yeast. (A) Increased Pmk1 phosphorylation in cells expressing a Cpc2(DE) version. Strains AN071 (*pmk1-HA6H leu1:cpc2-GFP*, *cpc2*Δ) and AN072 (*pmk1-HA6H leu1:cpc2(DE)-GFP*, *cpc2*Δ) were grown to mid-log phase in YES medium and treated with 0.6 M KCl for the indicated times. Pmk1-HA6H was purified by affinity chromatography under native conditions and the activated and total Pmk1 detected by immunoblotting with anti-phospho-p42/44 or anti-HA antibodies, respectively. (B) Decreased Pyp1 and Pyp2 protein levels in the Cpc2(DE) mutant. Strains AN091 (*leu1:cpc2-GFP cpc2*Δ *pyp1–13myc*) and AN092 (*leu1:cpc2(DE)-GFP cpc2*Δ *pyp1–13myc*) (*upper panel*), or AN102 (*leu1:cpc2-GFP cpc2*Δ *pyp2–13myc*) and AN103 (*leu1:cpc2(DE)-GFP cpc2*Δ *pyp2–13myc*) (*lower panel*) were grown in YES medium to mid-log-phase and treated with 0.6 M KCl. Aliquots were harvested at the times indicated and total extracts obtained. Pyp1–13myc or Pyp2–13myc fusions were detected by immunoblotting with anti-c-myc antibody. Anti-Cdc2 antibody was used for loading control. (C) Decreased Atf1 protein levels in the Cpc2(DE) mutant. Strains AN081 (*atf1-HA6H leu1:cpc2-GFP cpc2*Δ) and AN082 (*atf1-HA6H leu1:cpc2(DE)-GFP cpc2*Δ) were grown as above and treated with either 0.6 M KCl (top) or 1 mM H_2O_2 (bottom). Atf1 was purified by affinity chromatography from cell extracts of aliquots harvested at different time and detected by immunoblotting with anti-HA antibody. Anti-Cdc2 antibody was used for loading control. (D) *cpc2*Δ cells expressing the Cpc2(DE) version do not recover normal cell size at division. Cell morphology and size in strains AN100 (*cpc2*Δ), AN071 (*leu1:cpc2-GFP*, *cpc2*Δ), and AN072 (*leu1:cpc2(DE)-GFP*, *cpc2*Δ) growing in EMM2 medium and stained with calcofluor white are shown.

induced activation of MAPK Sty1 and MAPK Pmk1 are increased. Furthermore, in striking contrast with the mammalian model, *cpc2*$^+$ deletion triggers Pmk1 basal activity even in a *pck2*Δ background, suggesting that Cpc2 negatively regulates MAPK activity in fission yeast by a mechanism distinct from a role as Pck2 adaptor.

Which is the mechanism used by Cpc2 to regulate MAPK activity and to modulate cellular response against stress? In both human, budding and fission yeast cells RACK1/Asc1/Cpc2 associates with the 40S ribosomal subunit (Shor and McLeod, 2003; Baum *et al*., 2004; Coyle *et al*., 2009). Also, the study by Shor and McLeod (2003) demonstrated that the loss of *cpc2*$^+$ in *S. pombe* elicits a decreased steady state level of various proteins, some of which (like ribosomal protein L25) are probably regulated at the level of translation. The results presented in our work strongly support the interpretation that Cpc2 modulates the translation of a specific subset of mRNAs (Shor and McLeod, 2003). Probably, Cpc2 exerts its function as a positive translational regulator of mRNAs encoding Pyp1 and Pyp2 tyrosine phosphatases, which deactivate both Sty1 and Pmk1 (Madrid *et al*., 2007). Consistent with this hypothesis, Pyp1 and Pyp2 protein levels diminished in *cpc2*Δ cells growing exponentially or subjected to different stresses, although the expression of the corresponding mRNAs was not significantly affected by *cpc2*$^+$ deletion. Importantly, this translational control was specific for *pyp1*$^+$ and *pyp2*$^+$ mRNAs, because the protein levels of other phosphatases known to be involved in Sty1 and/or Pmk1 deactivation, such as Pmp1, Ptc1, or Ptc3, remained unchanged in the absence of Cpc2.

Alternatively, Cpc2 also regulates positively the translation of mRNA encoding the transcription factor Atf1. Atf1 is phosphorylated and stabilized by Sty1 MAPK to play a critical role in the response of *S. pombe* against a variety of stress conditions (Chen *et al*., 2003). Our results support, however, that the low levels of Atf1 protein observed in *cpc2*Δ cells do not compromise its function as a transcriptional activator in response to stress, because the induced expression of Atf1-dependent genes (including *pyp1*$^+$ and *pyp2*$^+$) in response to osmotic or oxidative stress was not

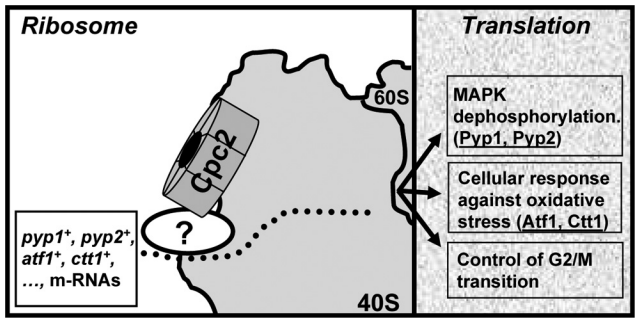

Figure 10. Proposed functional role for RACK orthologue Cpc2 in fission yeast. The Cpc2 protein regulates important biological processes at the ribosome level by favoring the translation of genes whose products may inactivate MAPK cascades (Pyp1 and Pyp2 MAPK phosphatases), enhance cellular defense against oxidative stress (transcription factor Atf1, cytoplasmic catalase Ctt1), and control G2/M transition of the cell cycle. The question mark highlights that the additional role of one or several proteins is not discarded.

significantly affected by *cpc2*$^+$ deletion. These data agree with previous work showing that there is still a robust transcriptional activation of Atf1-dependent genes in response to stress in a mutant strain expressing low levels of an unstable version of the transcription factor devoid of Sty1-phosphorylation sites (Lawrence *et al*., 2007). In this context, we have found that although the transcriptional induction of Atf1-dependent genes in *cpc2*Δ cells is not affected, Cpc2 regulates the cellular defense against hydrogen peroxide at a translational level by favoring the synthesis of detoxifying enzymes such as cytoplasmic catalase Ctt1. Probably, the synthesis of other detoxifying proteins may be also compromised in *cpc2*Δ cells.

The recent demonstration of the existence of conserved charged amino acids that are responsible for the in vivo Asc1/RACK1 association with the ribosome (Coyle *et al*., 2009) allowed our demonstration that the function of Cpc2 as a modulator of both the MAPK activity and the cellular response against oxidative stress relies on its ability for binding to the 40S subunit of the *S. pombe* ribosome. In addition, the putative role of Cpc2 in regulating the G2/M transition of the cell cycle seems to depend also on its function as a ribosomal protein. These results raise several important questions. One refers to the mechanism whereby Cpc2 regulates the recruitment and translation of specific mRNAs. Considering that Cpc2 lacks evident RNA binding motifs and taking into account the versatility of RACK1 as a platform to bind different proteins, it seems likely that one or several Cpc2 binding partners might be involved in the recruitment of specific mRNAs to the ribosome, as depicted in Figure 10. In *S. cerevisiae*, it has been described that Scp160, an mRNA binding protein orthologue to vertebrate vigilin, associates with ribosomes in an Asc1/RACK1-dependent manner, thus supporting that the Scp160-Asc1 complex mediates the translation activity of ribosomes programmed with specific mRNAs (Baum *et al*., 2004). The Scp160 orthologue in fission yeast is Vgl1, a putative mRNA binding protein with 12 KH domains. However, Vgl1-null cells do not display any of the phenotypes associated to Cpc2 deletion, such as increased cell length at G2/M transition or Pmk1 hyperactivation (unpublished data). Hence, it seems plausible that other unknown RNA binding protein(s) might be involved in this process. Another candidate to perform such role is RNA binding protein Msa2/Nrd1, which interacts in vivo with Cpc2 and whose deletion causes initiation of sexual development without nutrient starvation (Tsukahara *et al*., 1998; Jeong *et al*., 2004). Also, Msa2/Nrd1 binds and stabilizes Cdc4 mRNA, encoding myosin II light chain, and Nrd1 phosphorylation by Pmk1 negatively regulates its binding activity to Cdc4 mRNA (Satoh *et al*., 2009). However, the opposite roles described for Cpc2 and Msa2/Nrd1 in sexual differentiation (Jeong *et al*., 2004), together with the absence in Msa2-null cells of the main phenotypes associated to Cpc2 deletion, makes unlikely that this RNA-binding protein will be the Cpc2 binding partner involved in mRNA recruitment to the ribosome. A similar conclusion can be drawn in the case of Rnc1, another RNA-binding protein which is phosphorylated by Pmk1 and binds and stabilizes Pmp1 dual-specificity MAPK phosphatase involved in Pmk1 dephosphorylation (Sugiura *et al*., 2003). Our results clearly show that Pmk1-Rnc1 control of Pmp1 is independent on Cpc2, because the protein levels of Pmp1 remained unchanged in the absence of Cpc2. Regardless, the identification of the complete subset of mRNAs whose translation is positively regulated by Cpc2 (besides those described here), may deserve follow-up investigation. Our results provide for the first time strong evidence that a RACK1-type protein functions from the ribosome to control the magnitude of the activation of MAPK cascades, the cellular defense against oxidative stress, and the progression of the cell cycle, by regulating positively the translation of specific genes whose products are involved in key biological processes. On the basis of these data, we anticipate that some of the previously described biological functions of RACK1 in mammalian cells might be linked to its function as a putative translational regulator.

ACKNOWLEDGMENTS

We thank P. Pérez (Consejo Superior de Investigaciones Cientificas/University of Salamanca, Spain) for helpful discussions and comments on the manuscript; E. Boye (Institute for Cancer Research, Norway), T. Kato (ERATO, Japan), J. B. Millar (University of Warwick, United Kingdom), P. Pérez, M. A. Rodriguez-Gabriel (Universidad Autónoma, Madrid, Spain), and T. Toda (London Research Institute, United Kingdom) for kind supply of yeast strains; and F. Garro for technical assistance. Thanks to Javier Campoy (University of Murcia) for help and advice with polysome fractionation. A. N. is a predoctoral fellow from Fundación Séneca (Región de Murcia), Spain. A. F. is a postdoctoral fellow from the University of Murcia. This work was supported by grants BFU2008-01653 from Ministerio de Ciencia e Innovación and 08725/PI/08 from Fundación Séneca (Región de Murcia), Spain.

REFERENCES

Alfa, C., Fantes, P., Hyams, J., Mcleod, M., and Warbrick, E. (1993). Experiments with Fission Yeast. A Laboratory Course Manual, Cold Spring Harbor, NY: Cold Spring Harbor Laboratory Press.

Bahler, J., Wu, J. Q., Longtine, M. S., Shah, N. G., McKenzie, A. 3rd, Steever, A. B., Wach, A., Philippsen, P., and Pringle, J. R. (1998). Heterologous modules for efficient and versatile PCR-based gene targeting in *Schizosaccharomyces pombe*. Yeast *14*, 943–951.

Barba, G., Soto, T., Madrid, M., Núñez, A., Vicente, J., Gacto, M., and Cansado, J. (2008). Activation of the cell integrity pathway is channelled through diverse signalling elements in fission yeast. Cell. Signal. *20*, 748–757.

Baum, S., Bittins, M., Frey, S., and Seedorf, M. (2004). Asc1p, a WD40-domain containing adaptor protein, is required for the interaction of the RNA-binding protein Scp160p with polysomes. Biochem. J. *380*, 823–830.

Benko, Z., Sipiczki, M., and Carr, A. M. (1998). Cloning of *caf1*$^+$, caf2$^+$ and caf4$^+$ from *Schizosaccharomyces pombe*: their involvement in multidrug resistance, UV and pH sensitivity. Mol. Gen. Genet. *260*, 434–443.

Castillo, E. A., Ayté, J., Chiva, C., Moldón, A., Carrascal, M., Abián, J., Jones, N., and Hidalgo, E. (2002). Diethylmaleate activates the transcription factor Pap1 by covalent modification of critical cysteine residues. Mol. Microbiol. *45*, 243–254.

Chaudhuri, I., Soding, J., and Lupas, A. N. (2008). Evolution of the beta-propeller fold. Proteins *71*, 795–803.

Chen, D., Toone, W. M., Mata, J., Lyne, R., Burns, G., Kivinen, K., Brazma, A., Jones, N., and Bähler, J. (2003). Global transcriptional responses of fission yeast to environmental stress. Mol. Biol. Cell *14*, 214–229.

Coyle, S. M., Gilbert, W. V., and Doudna, J. A. (2009). Direct link between RACK1 function and localization at the ribosome in vivo. Mol. Cell. Biol. *29*, 1626–1634.

Degols, G., Shiozaki, K., and Russell, P. (1996). Activation and regulation of the Spc1 stress-activated protein kinase in *Schizosaccharomyces pombe*. Mol. Cell. Biol. *16*, 2870–2877.

Degols, G., and Russell, P. (1997). Discrete roles of the Spc1 kinase and the Atf1 transcription factor in the UV response of *Schizosaccharomyces pombe*. Mol. Cell. Biol. *17*, 3356–3363.

Higuchi, R., Krummel, B., and Saiki, R. K. (1988). A general method of in vitro preparation and specific mutagenesis of DNA fragments: study of protein and DNA interactions. Nucleic Acids Res. *16*, 7351–7367.

Hohmann, S. (2002). Osmotic stress signaling and osmoadaptation in yeasts. Microbiol. Mol. Biol. Rev. *66*, 300–372.

Jeong, H. T., Oowatari, Y., Abe, M., Tanaka, K., Matsuda, H., and Kawamukai, M. (2004). Interaction between a negative regulator (Msa2/Nrd1) and a positive regulator (Cpc2) of sexual differentiation in *Schizosaccharomyces pombe*. Biosci. Biotechnol. Biochem. *68*, 1621–1626.

Lawrence, C. L., Maekawa, H., Worthington, J. L., Reiter, W., Wilkinson, C. R., and Jones, N. (2007). Regulation of *Schizosaccharomyces pombe* Atf1 protein levels by Sty1-mediated phosphorylation and heterodimerization with Pcr1. J. Biol. Chem. *282*, 5160–5170.

Loewith, R., Hubberstey, A., and Young, D. (2000). Skh1, the MEK component of the mkh1 signaling pathway in *Schizosaccharomyces pombe*. J. Cell Sci. *113*, 153–160.

López-Bergami, P., Habelhah, H., Bhoumik, A., Zhang, W., Wang, L. H., and Ronai, Z. (2005). RACK1 mediates activation of JNK by protein kinase C. Mol Cell. *19*, 309–320.

Ma, Y., Kuno, T., Kita, A., Asayama, Y., and Sugiura, R. (2006). Rho2 is a target of the farnesyltransferase Cpp1 and acts upstream of Pmk1 mitogen-activated protein kinase signaling in fission yeast. Mol. Biol. Cell *17*, 5028–5037.

Madrid, M., Núñez, A., Soto, T., Vicente-Soler, J., Gacto, M., and Cansado, J. (2007). Stress-activated protein kinase-mediated down-regulation of the cell integrity pathway mitogen-activated protein kinase Pmk1 by protein phosphatases. Mol. Biol. Cell *18*, 4405–4419.

Madrid, M., Soto, T., Franco, A., Paredes, V., Vicente, J., Hidalgo, E., Gacto, M., and Cansado, J. (2004). A cooperative role for Atf1 and Pap1 in the detoxification of the oxidative stress induced by glucose deprivation in *Schizosaccharomyces pombe*. J. Biol. Chem. *279*, 41594–41602.

Madrid, M., Soto, T., Khong, H. K., Franco, A., Vicente, J., Pérez, P., Gacto, M., and Cansado, J. (2006). Stress-induced response, localization, and regulation of the Pmk1 cell integrity pathway in *Schizosaccharomyces pombe*. J. Biol. Chem. *281*, 2033–2043.

McCahill, A., Warwicker, J., Bolger, G. B., Houslay, M. D., and Yarwood, S. J. (2002). The RACK1 scaffold protein: a dynamic cog in cell response mechanisms. Mol. Pharmacol. *62*, 1261–1273.

McLeod, M., Shor, B., Caporaso, A., Wang, W., Chen, H., and Hu, L. (2000). Cpc2, a fission yeast homologue of mammalian RACK1 protein, interacts with Ran1 (Pat1) kinase to regulate cell cycle progression and meiotic development. Mol. Cell. Biol. *20*, 4016–4027.

Millar, J. B., Buck, V., and Wilkinson, M. G. (1995). Pyp1 and Pyp2 PTPases dephosphorylate an osmosensing MAP kinase controlling cell size at division in fission yeast. Genes Dev. *9*, 2117–2130.

Moreno, S., Klar, A., and Nurse, P. (1991). Molecular genetic analysis of fission yeast *Schizosaccharomyces pombe*. In: Methods in Enzymology, Vol. 283, New York: Academic Press, 506–520.

Nilsson, J., Sengupta, J., Frank, J., and Nissen, P. (2004). Regulation of eukaryotic translation by the RACK1 protein: a platform for signalling molecules on the ribosome. EMBO Rep. *5*, 1137–1141.

Quinn, J., Findlay, V. J., Dawson, K., Millar, J. B., Jones, N., Morgan, B. A., and Toone, W. M. (2002). Distinct regulatory proteins control the graded transcriptional response to increasing H(2)O(2) levels in fission yeast *Schizosaccharomyces pombe*. Mol. Biol. Cell *13*, 805–816.

Satoh, R., Morita, T., Takada, H., Kita, A., Ishiwata, S., Doi, A., Hagihara, K., Taga, A., Matsumura, Y., Tohda, H., and Sugiera, R. (2009). Role of the RNA-binding protein Nrd1 and Pmk1 mitogen-activated protein kinase in the regulation of myosin mRNA stability in fission yeast. Mol. Biol. Cell *20*, 2473–2485.

Sengupta, J., Nilsson, J., Gursky, R., Spahn, C. M., Nissen, P., and Frank, J. (2004). Identification of the versatile scaffold protein RACK1 on the eukaryotic ribosome by cryo-EM. Nat. Struct. Mol. Biol. *11*, 957–962.

Shiozaki, K., and Russell, P. (1995). Cell-cycle control linked to extracellular environment by MAP kinase pathway in fission yeast. Nature *378*, 739–743.

Shiozaki, K., and Russell, P. (1996). Conjugation, meiosis, and the osmotic stress response are regulated by Spc1 kinase through Atf1 transcription factor in fission yeast. Genes Dev. *10*, 2276–2288.

Shiozaki, K., and Russell, P. (1997). Stress-activated protein kinase pathway in cell cycle control of fission yeast. In: Methods in Enzymology, Vol. 283, New York: Academic Press, 506–520.

Shiozaki, K., Shiozaki, M., and Russell, P. (1998). Heat Stress activates fission yeast Spc1/Sty1 MAPK by a MEKK-independent mechanism. Mol. Biol. Cell *9*, 1339–1349.

Shor, B., and McLeod, M. (2003). Cpc2/RACK1 is a ribosome-associated protein that promotes efficient translation in *Schizosaccharomyces pombe*. J. Biol. Chem. *278*, 49119–49128.

Smith, T. F., Gaitatzes, C., Saxena, K., and Neer, E. J. (1999). The WD repeat: a common architecture for diverse functions. Trends Biochem. Sci. *24*, 181–185.

Soto, T., Beltrán, F .F., Paredes, V., Madrid, M., Millar, J.B.A., Vicente-Soler, J., Cansado, J., and Gacto, M. (2002). Cold induces stress-activated protein kinase-mediated response in the fission yeast *Schizosaccharomyces pombe*. Eur. J. Biochem. *269*, 1–10.

Sugiura, R., Toda, T., Shuntoh, H., Yanagida, M., and Kuno, T. (1998). $pmp1^{+}$, a suppressor of calcineurin deficiency, encodes a novel MAP kinase phosphatase in fission yeast. EMBO J. *17*, 140–148.

Sugiura, R., Kita, A., Shimizu, Y., Shuntoh, H., Sio, S. O., and Kuno, T. (2003). Feedback regulation of MAPK signalling by an RNA-binding protein. Nature *424*, 961–965.

Takada, H., *et al.* (2007). Atf1 is a target of the mitogen-activated protein kinase Pmk1 and regulates cell integrity in fission yeast. Mol. Biol. Cell *18*, 4794–4802.

Toda, T., Dhut, S., Superti-Furga, G., Gotoh, Y., Nishida, E., Sugiura, R., and Kuno, T. (1996). The fission yeast $pmk1^{+}$ gene encodes a novel mitogen-activated protein kinase homolog which regulates cell integrity and functions coordinately with the protein kinase C pathway. Mol. Cell. Biol. *16*, 6752–6764.

Tsukahara, K., Yamamoto, H., and Okayama, H. (1998). An RNA binding protein negatively controlling differentiation in fission yeast. Mol. Cell. Biol. *18*, 4488–4498.

Tvegård, T., Soltani, H., Skjølberg, H. C., Krohn, M., Nilssen, E. A., Kearsey, S. E., Grallert, B., and Boye, E. (2007). A novel checkpoint mechanism regulating the G1/S transition. Genes Dev. *15*, 649–654.

Vivancos, A. P., Castillo, E. A., Jones, N., Ayté, J., and Hidalgo, E. (2004). Activation of the redox sensor Pap1 by hydrogen peroxide requires modulation of the intracellular oxidant concentration. Mol. Microbiol. *52*, 1427–1435.

Vivancos, A. P., Jara, M., Zuin, A., Sansó, M., and Hidalgo, E. (2006). Oxidative stress in *Schizosaccharomyces pombe*: different H_2O_2 levels, different response pathways. Mol. Genet. Genomics *276*, 495–502.

Wilkinson, M. G., Samuels, M., Takeda, T., Toone, W. M., Shieh, J. C., Toda, T., Millar, J. B., and Jones, N. (1996). The Atf1 transcription factor is a target for the Sty1 stress-activated MAP kinase pathway in fission yeast. Genes Dev. *10*, 2289–2301.

Won, M., Park, S. K., Hoe, K. L., Jang, Y. J., Chung, K. S., Kim, D. U., Kim, H. B., and Yoo, H. S. (2001). Rkp1/Cpc2, a fission yeast RACK1 homolog, is involved in actin cytoskeleton organization through protein kinase C, Pck2, signaling. Biochem. Biophys. Res. Commun. *282*, 10–15.

Yamada, K., Nakagawa, C. W., and Mutoh, N. (1999). *Schizosaccharomyces pombe* homologue of glutathione peroxidase, which does not contain selenocysteine, is induced by several stresses and works as an antioxidant. Yeast *15*, 1125–1132.

Yoshida, T., Toda, T., and Yanagida, M. (1994). A calcineurin-like gene $ppb1^{+}$ in fission yeast: mutant defects in cytokinesis, cell polarity, mating and spindle pole body positioning. J. Cell Sci. *107*, 1725–1735.

Zaitsevskaya-Carter, T., and Cooper, J. A. (1997). Spm1, a stress-activated MAP kinase that regulates morphogenesis in *S. pombe*. EMBO J. *16*, 1318–1331.

Zhan, K., Vattem, K. M., Bauer, B. N., Dever, T. E., Chen, J. J., and Wek, R. C. (2002). Phosphorylation of eukaryotic initiation factor 2 by heme-regulated inhibitor kinase-related protein kinases in *Schizosaccharomyces pombe* is important for resistance to environmental stresses. Mol. Cell. Biol. *22*, 7134–7146.